

NASA Contractor Report 168247

TEMPERATURE HISTORIES OF COMMERCIAL FLIGHTS
AT SEVERE CONDITIONS FROM GASP DATA

W. H. Jaspersen and G. D. Nastrom

Control Data Corporation
Minneapolis, Minnesota

October 1983

Prepared for

NATIONAL AERONAUTICS AND SPACE ADMINISTRATION
Lewis Research Center
Under Contract NAS3-21249

1.0 SUMMARY

This report is a study of the thermal environment of commercial aircraft from a data set gathered during the Global Atmospheric Sampling Program (GASP). The data set covers a four-year period of measurements. The report presents plots of airplane location and speed and atmospheric temperature as functions of elapsed time for 36 extreme-condition flights, selected by minimum values of several temperature parameters. One of these parameters, the severity factor, is an approximation of the in-flight wing-tank temperature. Representative low-severity-factor flight histories may be useful for actual temperature-profile inputs to design and research studies. Comparison of the GASP atmospheric temperatures to interpolated temperatures from National Meteorological Center and Global Weather Central analysis fields shows that the analysis temperatures are slightly biased toward warmer than actual temperatures, particularly over oceans and at extreme conditions.

2.0 INTRODUCTION

By most criteria, aircraft fly in a hostile environment. In particular, commercial aircraft typically fly at heights where the outside air temperature may be -70°C or colder. Present aviation turbine fuels have low freezing points to insure flowability at minimum temperatures. However, fuels with higher freezing points can allow better future utilization of scarce and changing raw materials and flexibility in meeting changes in product demands.

Engineers have the option of modifying aircraft fuel systems so that the fuel is not subjected to as severe a temperature stress. This may be done passively by altering the exposure or actively by heating the tanks (refs. 1-3). If either of these alternatives is considered, there has to be a balance between the effectiveness and the penalties paid in terms of cost complexity, maintainability, weight and aircraft performance.

In order to evaluate potential fuel system modifications, through design or experimental studies, representative extreme-environment flights must be characterized. Figure 1 presents the average air temperature as a function of latitude and height (ref. 4). As expected, the temperature decreases poleward in the lower atmosphere. However, above approximately 14 km (46000 ft) in winter (figure 1[a]) and 12 km (40000 ft) in summer (figure 1[b]), the average temperature decreases equatorward with the result that the coldest average temperatures found in the atmosphere are at approximately 17 km (54000 ft) over the equator.

The day-to-day fluctuations in atmospheric temperatures are far more important in relationship to minimum fuel temperatures and flowability than are the mean temperatures. Previous studies have compiled statistics on minimum atmospheric temperatures to determine the probability of occurrence of extremes. In one study, a survey of 8125 flights over 12 commercial routes gave the probability distribution of minimum fuel, total air, and static air temperatures (ref. 5). Actual flight histories and the time of occurrence of minima were not reported. Flight temperature histories were constructed for several military missions in another study, using National Meteorological Center analysis field data over a ten-year period with heat transfer model calculations (ref. 6).

This present study utilizes a set of temperature data collected on many routes worldwide. A previous report (ref. 7) presented statistical data from each flight and organized the observed atmospheric temperatures into probability tables by monthly geographic and altitude grids. The current study presents complete temperature histories of selected flights determined to be most extreme according to several parameters. One of these parameters is a severity factor, an approximation of the wing-tank fuel temperature. The analysis of temperatures includes comparisons of temperatures measured by the aircraft and temperatures interpolated from analysis fields.

3.0 DATA

The NASA Global Atmospheric Sampling Program (GASP) ran from March 1975 to July 1979. During this program four commercial B747 aircraft in routine service were instrumented to obtain measurements of aerosols, trace constituents and meteorological variables (refs. 8 and 9). The GASP system was automated to record data at nominal five-minute intervals during flight above FL190 (5.8 km or 19000 ft according to the ICAO Standard Atmosphere). When turbulence was encountered, or on entire selected flights, data were recorded at four-second intervals (ref. 10), but for this study only one-minute interval data were retained. Temperatures were measured with a Rosemount temperature sensor for which the expected rms error is less than 1°C (ref. 11). The temperature data, however, were recorded in whole degrees Celsius.

The data set used in this study consists of 6945 flights covering 273 different routes. Most of these routes are in the United States (including Hawaii) or are from the U. S. to Europe or Japan. However, there also are numerous flights from the Northern Hemisphere to the Southern Hemisphere, within the Southern Hemisphere, between cities along the southern rim of Asia, and even into Africa. Airport codes and locations are listed in Table 1. A complete summary of all GASP flights is found in ref. 7.

Analysis fields of temperature produced by the National Meteorological Center (NMC) and by the Air Force Global Weather Central (GWC) were also used in this study. Both data sets are gridded on a 1977-point octagon presented in fig. 2. Both data sets cover the Northern Hemisphere to about 18°N latitude. These gridded data are available twice a day, at 0000 GMT and 1200 GMT, and the following pressure levels were used:

- 500 mb (50 kPa pressure, corresponding to 5.6 km, FL180)
- 400 mb (7.2 km, FL240)
- 300 mb (9.2 km, FL300)
- 250 mb (10.4 km, FL340)
- 200 mb (11.8 km, FL390)
- 150 mb (13.6 km, FL450)
- 100 mb (16.2 km, FL530)

4.0 ANALYSIS OF DATA

4.1 Selection Parameters

Five different temperature severity parameters were defined and computed for each of the 6945 GASP flights to select flights that met criteria for coldest temperatures. These parameters are defined as follows:

4.1.1 Minimum Temperature

The minimum temperature is the minimum or most extreme single event ambient (static) temperature recorded at any time during the flight.

4.1.2 Thermal Exposure

The thermal exposure is the time weighted sum of the ambient temperatures encountered over the entire flight, expressed in units of degree-minutes. Mathematically it is given by

$$E = \sum_{t=1}^{t=n} T_S \Delta t$$

where E is the thermal exposure,

T_S is the ambient (static) temperature,

Δt is the time interval,

and t is the number of the time interval from the start of cruise (t=1) to the end of cruise (t=n).

4.1.3 Average Temperature

The average temperature for a flight is the thermal exposure divided by the total time duration of the flight.

4.1.4 Severity Factor

The severity factor is an estimate of the fuel temperature during the flight, not measured by the GASP instrumentation. The severity factor is calculated by assuming a time-varying heat transfer coefficient. The coefficient is based on Boeing calculations for configurations typical of the GASP aircraft (ref. 12). Mathematically, the severity factor is given by:

$$T_{sf,i} = T_{sf,i-1} - K(T_{sf,i-1} - T_{r,i})\Delta t$$

where $T_{sf,i}$ is the severity factor after time interval i ,
 K is the thermal constant (assumed to be $7.84 \times 10^{-3} \text{ min}^{-1}$),
 $T_{sf,i-1}$ is the severity factor after time interval $i-1$,
 $T_{r,i}$ is the recovery temperature during time interval $i-1$,
and Δt is the time interval.

The recovery temperature is given by

$$T_{r,i} = (1 + 0.18M_i^2) T_{s,i}$$

where M_i is the Mach number over interval i ,
and $T_{s,i}$ is the static air temperature over interval i . This equation assumes an adiabatic recovery of 90%.

The severity factor at the start of cruise, $T_{sf,0}$, was assumed to be -17°C .

4.1.5 Minimum Average Segment Temperature

A flight segment is defined as a portion of a flight in excess of two hours duration during which the flight level changes by less than $\pm 150\text{m}$ (500 ft). If more than one such segment exists, this parameter is the one with the coldest average temperature.

4.2 Coldest Flights

The computation of each of these parameters for all GASP flights resulted in an ordered set of flights from most severe to least severe for each parameter. From this set, 36 "most severe" flights were selected. These flights are shown in Table 2 along with the values of the selection parameter. The flights are ranked in Table 2 in a general order of decreasing severity. The order is subjective, but flights were judged more severe if they were extreme in more than one of the selection parameters. Nineteen different airport pairs are represented in Table 2. The most consistently severe route is between Bahrain Island in the Arabian Gulf or Dhahrain, Saudi Arabia, and New York. Seven of the 36 flights are between these cities.

5.0 DISCUSSION OF DATA

5.1 Flight Histories

Flight histories of the 36 selected flights of Table 2 are presented in the order of rank in figs. 3 to 38. Each of these figures is a panel with multiple plots of recorded and calculated parameters as common functions of flight duration.

Each panel is labeled across the top with the airports of departure and destination, the time of the first data point (time of departure), and the date of the flight. Within each panel, there are seven sets of plots with separate ordinates alternated between the left and right margins. All refer to the common abscissa of elapsed time. From the bottom up, the plots show aircraft speed (Mach number), altitude (flight level), distance from the NMC tropopause (where available), static air temperature, severity factor (approximate fuel temperature), latitude and longitude. Distance may be estimated by the nominal equivalence of 1700 km, or 1000 statute miles to each 100 minutes of elapsed time.

All GASP data were measured from Boeing 747 aircraft, and the average cruising speeds fluctuate about Mach 0.85. The flight level, or pressure altitude of the aircraft, is determined by all of the variables that go into the flight plan and ranges from 10 to 13 km (33000 to 43000 ft).

The height of the NMC tropopause was interpolated to each recorded aircraft position from NMC tropopause analysis fields, and the height difference between the tropopause and the aircraft is plotted in the panel in pressure units (mb). A positive distance indicates that the aircraft is above the tropopause. Tropopause data were available for most northern hemisphere flights.

The static air temperature as recorded by the aircraft is presented in the next part of the panel. If NMC and/or GWC temperature data were also available, they are also included on the same scale as the GASP temperatures. The NMC (GWC) temperature curve is distinguished from the others by small boxes (triangles) drawn at 100 minute intervals. The NMC and GWC temperature data were interpolated from the gridded fields to the aircraft position linearly with respect to horizontal distance and time and linearly with respect to the logarithm of pressure in the vertical.

The severity factor, or arbitrary fuel temperature, is included above the temperature curve. The severity factor, defined in section 4.1.4, can be seen to represent a damped response to the air temperature (or, more specifically, the recovery temperature). The top plots in each panel are the flight location, longitude and latitude, as functions of elapsed time.

5.2 Severity Factors

Temperature patterns in the atmosphere are reflections of meridional circulation patterns. Near the earth's surface in midlatitudes, the primary circulation features are sequences of high pressure and low pressure systems imbedded in the westerly winds. In the upper atmosphere,

say above 6 km (20000 ft), these pressure systems appear as meridional deviations or waves in a basically zonal (west to east) flow. An aircraft will generally encounter, during any season of the year, sequences of relatively high and relatively low temperatures. An examination of the flight histories presented in figures 3 to 38 shows that cold areas tend to have a duration of 100 to 200 minutes (1000 to 2000 miles). What this implies is that even though ambient air temperatures may occasionally reach -70°C or colder, they do not remain at that extreme level over an entire long flight. It also shows why it is important to look at actual flight histories, either measured or inferred from analysis fields, rather than simple temperature-altitude climatologies when examining a thermal exposure problem.

The severity factor is calculated from the air temperature and appears as a damped response to the flight temperature variations. The minimum value of the severity factor is not directly related to the average air temperature along the route. The magnitude and duration of any deviation from the average is more important. Furthermore, cold air temperatures late in a flight will tend to produce more extreme severity factors than cold temperatures early in a flight.

A demonstration of the relationship of severity factor to wing-tank fuel temperature is shown by the comparison in figure 39 of calculated severity factors for a published flight history of a flight from Seattle to Johannesburg (ref. 2). The severity factor assumes an initial fuel temperature of -17°C ; in the comparison flight, the initial temperature was -8°C . However, the influence of initial fuel temperature becomes negligible after several hours of flight time (compare ref. 12). Both the severity factor and the Boeing prediction model approximate the measured fuel temperature well. The severity factor is based on the Boeing technique with an arbitrary initial temperature and other simplifications.

The severity factors presented in the flight histories were calculated from the GASP temperatures. Table 3 compares the minimum severity factors

from Table 2 for the selected flights as calculated from the GASP temperatures with the factors calculated from the NMC and/or GWC data, if available. It is significant to note that in only one case was the severity factor computed from analysis fields colder than the severity factor computed from the aircraft measured temperatures, and this was by only 0.03°C (flight rank 11). In general, the severity factors computed from the analysis fields were 3 to 5°C warmer than the GASP severity factors. The differences appear to be due primarily to the fact that the analysis fields tend to be consistently biased toward warmer temperatures during the coldest portions of the flights. Because most of the flights are over water, it is difficult to judge if this bias is due to the fact that there are less input data over the oceans or due to a damping or averaging bias. One of the few flights completely over land (rank 13) also shows a bias between the temperatures. In any case, one should be aware of the magnitude of the differences in minimum severity factor that can result from different types of input data.

On the basis of severity factor and the other parameters, five routes that were generally the coldest were identified from among the 19 represented by the selected flights. These routes and the number of flights available are:

Los Angeles (LAX) - Tokyo (HND,NRT)	234
San Francisco (SFO) - Hong Kong (HKG)	51
San Francisco (SFO) - Auckland (AKL)	36
New York (JFK) - Bahrain Is. (BAH)	43
New York (JFK) - Rio de Janeiro (GIG)	30

The average temperature and severity factor were computed for each flight, and the empirical probabilities of occurrence for several selected probabilities were determined. These empirical values are presented in Table 4.

A criterion of extreme temperature conditions often used for design and research is that of a one-day-a-year probability (refs. 5 and 12).

Two of the coldest routes, JFK-BAH and LAX-Tokyo, do have minimum severity factors and average temperatures which are normally distributed. With an assumption of normality, the one-day-a-year probability on these two routes can be estimated:

<u>Route</u>	<u>Minimum Severity Factor, °C</u>	<u>Average Temperature, °C</u>
JFK, BAH	-42.3	-63.6
LAK, Tokyo	-39.8	-62.5

Thus the rank 1 temperature history (figure 3) corresponds closely to a one-day-a-year flight profile with respect to the minimum severity factor. Other temperature histories of figures 3 to 38 may also be useful as representative of actual low-probability, extreme-condition flights, adapted and modified as necessary.

5.3 Further NMC, GWC and GASP Temperature Comparisons

It should be noted that changes in flight level produce corresponding changes in the distances from the tropopause, the temperatures, and occasionally the aircraft speed. Apart from the near discontinuities in these flight histories due to flight level changes, the plots of the distance from the NMC tropopause and the NMC and GWC temperature curves should be smooth. The distance between analysis field grid points is equivalent to about 25 minutes of flight time at normal cruise speeds. This implies that features in the temperature field with wave lengths smaller than about 50 minutes of flight time cannot be represented by the NMC/GWC analysis fields. Much more structure is resolvable in the GASP data which are taken, for the most part, at five-minute intervals. Even if allowance is made for the damping of temperature details, there are often significant differences between the GASP temperatures and the NMC/GWC analysis fields. Furthermore, there are also instances where there are large differences between the NMC and the GWC temperatures.

Upper air data have historically been much more readily available over land than over the oceans. With satellites, more data have been made available over the oceans, but it is still generally conceded that the quality and detail of the data over land exceeds that of data over the oceans. For this reason, two routes, one over land and one over the ocean, were selected to compare the temperature analysis fields with the GASP temperatures. The land route was between New York and San Francisco (146 flights), and the oceanic route was between San Francisco and Tokyo (108 flights).

Figure 40(a) presents the distribution of the differences between GASP and NMC temperatures for the oceanic flights and the continental flights. The continental flight temperature differences have a mean almost equal to zero and a standard deviation of 1.65°C . The oceanic flights, on the other hand, have a mean difference bias of 0.85°C and a standard deviation of 3.55°C . The mean difference is such that the NMC temperatures are warmer than the GASP temperatures, thereby understating the severity. Figure 40(b) shows the distribution of the probability that the absolute value of the temperature difference will be exceeded. The greater spread of the oceanic flight differences is apparent.

Figure 41 presents a comparison between GASP/NMC temperatures and GASP/GWC temperatures for both oceanic and continental routes. Only flights for which both NMC and GWC temperature data were available were used. Statistical differences between the NMC and GWC temperatures for either route are small. The positive temperature bias for the oceanic route and the slight negative bias for the continental route are evident.

Figure 42(a) presents the distribution of the GASP and NMC temperature differences for the oceanic flights (same as figure 40[a]) and the distribution of the GASP and NMC temperature differences for the selected flights of Table 2 for which NMC data were available. This figure is interesting in two respects. First, a much larger mean

temperature difference bias (1.65°C) is apparent in the coldest flight data set. This fact reiterates the point that the temperature analysis fields will underestimate the thermal severity of an actual flight. Secondly, the bias difference is not reflected in fig. 42(b) which shows the distribution of the probability that the absolute value of the temperature difference will be exceeded. Cumulative distributions like fig. 42(b) are often used to estimate error bounds, and the fact that these two are nearly identical occurs in this case by chance. This example serves to illustrate that care must be taken in interpreting results when absolute values are used in transforming a probability distribution to a cumulative distribution.

6.0 SUMMARY OF RESULTS

This report has presented a study of the thermal environment of commercial aircraft from a data set gathered during the Global Atmospheric Sampling Program. This data set consists of 6945 flights covering 273 routes over most of the world.

From the analysis of this data set, the following results are obtained.

1. Thirty-six flights, representing 19 different routings, were selected by several temperature parameters as the most severe. This report includes plots of airplane position, speed, and atmospheric temperature as functions of elapsed time for each of the selected flights. A table shows the various minimum temperature parameters for each selected flight.

2. A severity factor is defined as one of the representative extreme temperatures. This factor may be used to select worst case low-probability flights for design and research modeling. The severity factor is an approximation of the wing-tank temperature, related to the minimum enroute temperatures, their duration, and time of occurrence during flight.

3. Ambient temperatures as measured from the aircraft were compared with the temperature interpolated from National Meteorological Center (NMC) and Global Weather Central (GWC) analysis fields, and it was found that the interpolated temperatures were slightly biased towards warmer than actual temperatures. This was particularly true over the oceans and for the thermally severe flights. NMC and GWC gridded data appeared statistically similar.

7.0 REFERENCES

1. Pasion, A. J.: Design and Evaluation of Aircraft Heat Source Systems for Use with High-Freezing Point Fuels. NASA CR-159568, 1979.
2. Thomas, I.: Broadened Jet Fuel Specifications: Their Effect upon Commercial Airplane Design and Operation. Shell Aviation News, No. 450, pp. 32-35, 1978.
3. McConnell, P. M., L. A. Desmarais, G. N. Peterson, and C. L. Delaney: Operational Effects of Increased Freeze Point Fuels in Military Airplanes. AIAA Paper AIAA-83-1139, June 1983.
4. Byers, H. R.: General Meteorology. New York: McGraw Hill, 1959.
5. Pasion, A. J.: In-flight Fuel Tank Temperature Survey Data. NASA CR-159569, 1979.
6. McConnell, P. M., L. A. Massmann, G. N. Peterson, and F. F. Tolle: Fuel/Engine/Airplane Trade Off Study, Operational Effects of Increased Freeze Point Fuels. AFWAL-TR-82-2067, 1982.
7. Nastrom, G. D., and W. H. Jasperson: Flight Summaries and Temperature Climatology at Airliner Cruise Altitudes from GASP Data. NASA CR-168106, 1983.
8. Perkins, P. J.: Global Measurements of Gaseous and Aerosol Trace Species in the Upper Troposphere and Lower Stratosphere from Daily Flights of 747 Airliners. NASA TM X-73544, 1976.
9. Perkins, P. J., and L. C. Papathakos: Global Sensing of Gaseous and Aerosol Trace Species Using Automated Instrumentation on 747 Airliners. NASA TM-73810, 1977.

10. Holdeman, J. D. and E. A. Lezberg: NASA Global Atmospheric Sampling Program (GASP) Data Report for Tape VL0001. NASA TM X-71905, 1976.
11. Stickney, T. M., M. W. Shedlov, D. I. Thompson and F. J. Yakos: Rosemount Total Temperature Sensors Technical Report 5755, Revision A. Rosemount, Inc., Mpls., MN, 1981.
12. Pasion, A. J., and I. Thomas: Preliminary Analysis of Aircraft Fuel Systems for Use with Broadened Specification Fuels. NASA CR-135198, 1977.

TABLE 1
Airport/City Codes and Locations

<u>CITY</u>	<u>LAT.</u>	<u>LONG.</u>
ACA - Acapulco, Mexico	16.75N	99.76W
AKL - Auckland, New Zealand	37.03S	174.81E
AMS - Amsterdam, Netherlands	52.30N	4.76E
ANC - Anchorage, Alaska	61.17N	149.98W
ATH - Athens, Greece	37.96N	23.73E
BAH - Bahrain Is., Arabian Gulf	26.00N	50.60E
BDA - Bermuda, Atlantic Ocean	32.36N	64.63W
BEG - Belgrade, Yugoslavia	44.82N	20.30E
BEY - Beirut, Lebanon	33.82N	35.49E
BGR - Bangor, Maine	44.81N	68.82W
BKK - Bangkok, Thailand	13.90N	100.60E
BNE - Brisbane, Australia	27.44S	153.12E
BOM - Bombay, India	19.15N	72.86E
BOS - Boston, Mass.	42.36N	71.01W
BRU - Brussels, Belgium	50.90N	4.49E
CCS - Caracas, Venezuela	10.62N	66.97W
CGN - Cologne, Germany	50.93N	7.32E
CHC - Christchurch, New Zealand	43.51S	172.52E
CLE - Cleveland, Ohio	41.41N	81.84W
CPH - Copenhagen, Denmark	55.54N	12.81E
CPT - Capetown, South Africa	33.90S	18.68E
CTS - Sapporo, Japan	42.80N	141.67E
CUN - Cancun, Mexico	21.03N	86.88W
CUR - Curacao, Neth. Antilles	12.25N	68.91W
DAM - Damascus, Syria	33.50N	36.50E
DEL - Delhi, India	28.56N	77.12E
DEN - Denver, Colorado	39.76N	104.89W
DFW - Dallas/Ft. Worth, Texas	32.88N	97.03W
DHA - Dhahrain, Saudi Arabia	26.28N	50.17E
DRW - Darwin, Australia	12.36S	130.89E
DTW - Detroit, Michigan	42.24N	83.39W
DUB - Dublin, Ireland	53.44N	6.26W
EZE - Buenos Aires, Argentina	34.81S	58.53W
FAI - Fairbanks, Alaska	64.82N	147.86W
FCO - Rome, Italy	41.80N	12.25E
FRA - Frankfurt, Germany	50.05N	8.58E
GIG - Rio de Janeiro, Brazil	22.84S	43.20W
GUA - Guatemala City, Guatemala	14.59N	90.52W
GUM - Guam Island, Mariana Islands	13.41N	144.80E
HKG - Hong Kong, Hong Kong	22.33N	114.21E
HND - Tokyo, Japan	35.54N	139.77E
HNL - Honolulu, Hawaii	21.33N	157.92W
IAD - Washington, D.C.	38.94N	77.44W
IAH - Houston, Texas	29.49N	95.28W
IST - Istanbul, Turkey	40.98N	28.83E

TABLE 1 (cont'd)

ITO - Hilo, Hawaii	19.64N	155.03W
JFK - New York, New York	40.63N	73.77W
JNB - Johannesburg, South Africa	26.12S	28.22E
KHI - Karachi, Pakistan	24.90N	67.15E
KUL - Kuala Lumpur, Malaysia	3.12N	101.66E
LAS - Las Vegas, Nevada	36.08N	115.15W
LAX - Los Angeles, California	33.95N	118.40W
LHR - London, England	51.47N	.43W
LPA - Las Palmas, Canary Island	27.94N	15.39W
MEL - Melbourne, Australia	37.67S	144.84E
MEX - Mexico City, Mexico	19.45N	99.05W
MIA - Miami, Florida	25.79N	80.27W
MIQ - Caracas, Venezuela	10.60N	66.99W
MNL - Manila, Philippines	14.49N	121.02E
MRU - Mauritius, Indian Ocean	20.45S	57.68E
MUC - Munich, Germany	48.08N	11.60E
NAN - Nandi, Fiji Island	17.75S	177.46E
NCE - Nice, France	43.57N	7.41E
NOU - Noumea, New Caledonia	22.01S	166.24E
NRT - Tokyo, Japan	35.72N	140.32E
OKA - Okinawa, Japan	26.20N	127.63E
OMA - Omaha, Nebraska	41.34N	95.89W
ORD - Chicago, Illinois	41.97N	87.90W
OSA - Osaka, Japan	34.78N	135.42E
ORY - Paris, France	48.77N	2.38E
PDX - Portland, Oregon	45.85N	122.47W
PER - Perth, W. Australia	31.92S	115.94E
PHL - Philadelphia, Pennsylvania	39.90N	75.07W
PIK - Glasgow, Scotland	55.60N	4.70W
PPG - Pago Pago, Samoa	14.06S	170.68W
PPT - Papeete, Tahiti	17.55S	149.60W
PTY - Panama City, Panama	9.08N	79.38W
SEA - Seattle, Washington	47.44N	122.30W
SFO - San Francisco, California	37.61N	122.39W
SIN - Singapore, Singapore	1.44N	103.85E
SNN - Shannon, Ireland	52.69N	8.91W
STL - St. Louis, Missouri	38.75N	90.36W
STR - Stuttgart, Germany	48.55N	9.21E
SYD - Sydney, Australia	33.87S	151.34E
THR - Tehran, Iran	35.68N	51.31E
TPE - Taipei, Taiwan	25.07N	121.54E
VIE - Vienna, Austria	48.11N	16.58E
YQX - Gander, Newfoundland, Canada	48.98N	54.50W
YVR - Vancouver, B.C. Canada	49.20N	123.18W
YYZ - Toronto, Ontario, Canada	43.67N	79.61W

Table 2

Selected Extreme Condition Flights

Rank	Departure- Destination Airports	Date	Parameter Values				
			Min Temp, °C	Thermal Exposure °C-Min	Avg Temp, °C	Min Severity Factor, °C	Avg Segment Temp °C
1	BAH-JFK	11/25/78	-73	-46840	-60.1	-42.5	-70.8
2	CPT-AKL	10/29/77	-72	-47693	-59.0	-39.7	-66.9
3	BAH-JFK	1/ 3/79	-73	-46968	-59.1	-38.5	-66.3
4	JFK-DFW	5/ 2/77	-71	-9755	-65.9	-32.7	-67.8
5	SIN-HKG	11/29/78	-71	-10801	-65.5	-34.9	-70.0
6	SNN-JFK	1/27/76	-71	-24262	-64.4	-40.7	-69.7
7	FRA-JFK	1/ 2/79	-71	-28838	-63.7	-37.5	-67.0
8	SFO-HNL	4/12/75	-68	-17661	-64.9	-37.1	-67.0
9	NRT-SFO	2/ 4/79	-74	-28172	-58.2	-37.4	-61.8
10	JFK-DHA	2/22/79	-73	-38025	-58.4	-37.4	-62.6
11	JFK-HND	12/16/77	-68	-48168	-59.4	-35.3	-62.7
12	BOM-BAH	11/25/78	-69	-11175	-65.7	-34.2	-67.8
13	DFW-JFK	5/ 4/77	-70	-8520	-65.5	-31.0	----
14	HND-LAX	3/ 2/77	-74	-30416	-59.5	-35.7	-62.0
15	HND-LAX	2/16/78	-73	-27595	-56.9	-33.9	-61.8
16	JFK-BAH	1/25/77	-73	-37870	-58.7	-33.4	-58.2
17	LAX-HND	12/17/77	-73	-37255	-56.4	-36.9	-57.2
18	LHR-JFK	1/26/76	-69	-22157	-63.9	-38.7	----
19	ORD-HNL	4/ 4/79	-68	-29817	-61.9	-38.7	-65.7
20	JFK-HND	10/18/76	-66	-45920	-57.6	-32.6	-59.3
21	BAH-JFK	11/23/78	-69	-45910	-58.6	-34.5	-59.5
22	GIG-JFK	3/28/77	-71	-31675	-59.8	-38.9	-69.2
23	SYD-SFO	5/22/77	-67	-40745	-55.4	-37.2	-66.1
24	PPT-PPG	5/10/77	-67	-9667	-64.0	-31.9	-66.3
25	HKG-SIN	12/10/77	-66	-10920	-62.4	-31.9	-65.1
26	SFO-HKG	12/ 9/77	-64	-45556	-54.4	-34.0	-63.2
27	DHA-JFK	2/24/79	-69	-45348	-56.9	-34.5	-61.8
28	HND-LAX	4/18/77	-71	-30840	-60.8	-37.2	-62.7
29	HKG-SFO	4/11/79	-70	-36620	-56.8	-37.2	-64.0
30	SFO-AKL	12/25/76	-70	-42156	-57.0	-37.2	-60.3
31	SFO-HKG	5/29/78	-64	-42787	-51.2	-31.2	-61.7
32	SYD-SFO	7/ 3/77	-67	-44615	-56.8	-35.7	-64.6
33	LAX-HND	4/19/77	-68	-40562	-61.3	-35.3	-67.3
34	DHA-JFK	2/22/79	-72	-41910	-54.7	-36.6	-63.3
35	HND-JFK	2/14/77	-72	-35482	-53.3	-30.6	-62.0
36	JFK-HND	5/16/78	-64	-39151	-53.5	-32.9	-55.7

Table 3

Comparison of Minimum Severity Factors of Selected Flights

<u>Rank</u>	<u>SF*</u> <u>GASP</u>	<u>SF*</u> <u>NMC</u>	<u>SF*</u> <u>GWC</u>
1	-42.46	-35.59	-
2	-40.22	-	-
3	-38.47	-33.88	-
4	-32.67	-29.97	-
5	-34.88	-	-
6	-40.77	-36.53	-
7	-37.48	-35.25	-
8	-37.09	-	-
9	-37.39	-33.46	-32.08
10	-37.39	-31.64	-33.59
11	-35.26	-35.23	-35.29
12	-34.15	-29.77	-
13	-31.00	-28.28	-
14	-35.65	-32.42	-
15	-33.89	-33.14	-30.08
16	-33.45	-	-
17	-36.91	-31.40	-33.16
18	-38.74	-33.16	-
19	-38.74	-	-
20	-32.60	-30.73	-
21	-34.49	-37.10	-
22	-38.87	-	-
23	-37.21	-	-
24	-31.91	-	-
25	-32.96	-	-
26	-33.99	-30.98	-31.84
27	-34.49	-32.89	-33.63
28	-37.22	-35.81	-34.04
29	-37.22	-33.80	-32.87
30	-37.36	-	-
31	-31.71	-28.30	-
32	-35.65	-	-
33	-35.32	-32.84	-31.44
34	-36.56	-32.86	-32.79
35	-30.60	-28.91	-29.95
36	-32.90	-29.46	-

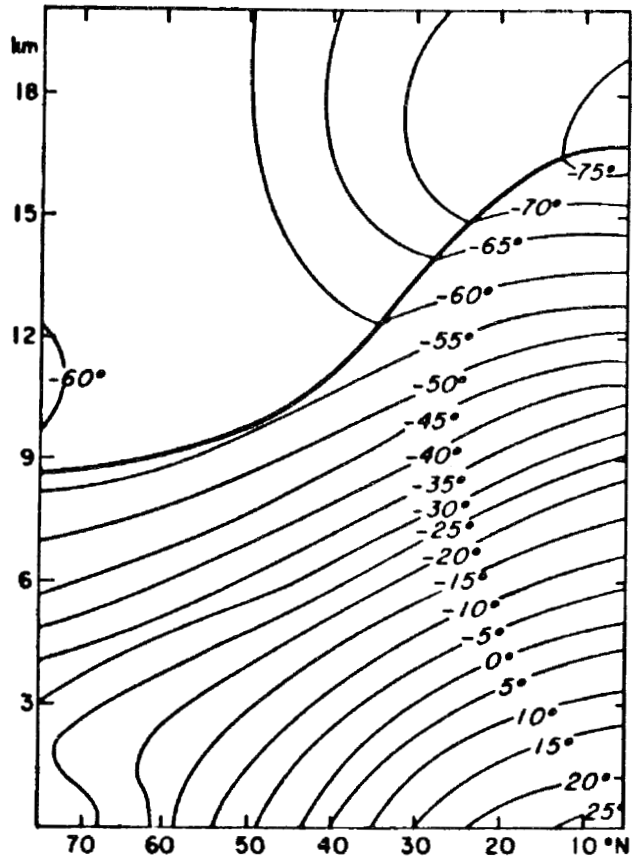
* SF_{GASP}, SF_{NMC}, and SF_{GWC} are the minimum severity factors as computed from the GASP temperature and the NMC and GWC analysis fields, respectively.

Table 4.

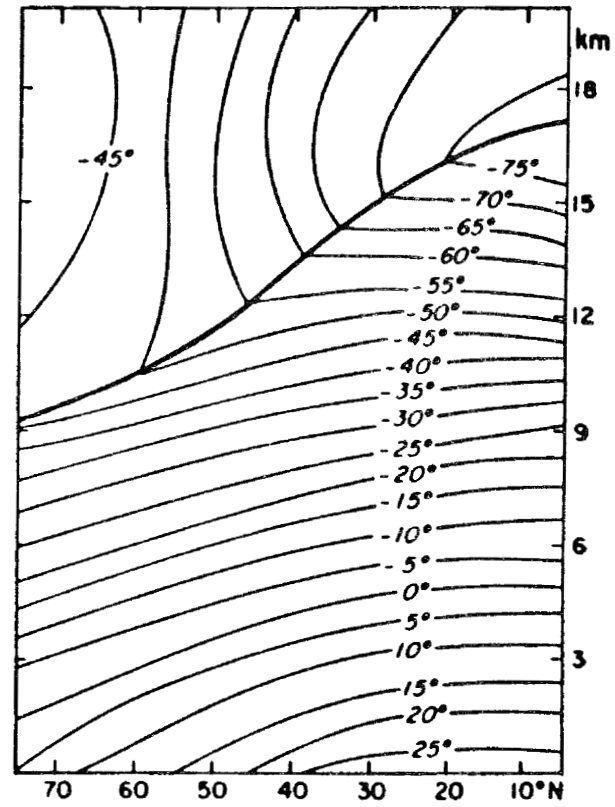
Probability of Occurrence for Two Temperature Parameters on Five Coldest Routes

Route	Probability	<u>Severity Factor, °C</u>							
		1%	5%	10%	25%	50%	75%	90%	95%
JFK, BAH	-	-38.0	-35.5	-33.7	-31.5	-29.0	-26.3	-25.0	-
GIG, JFK	-	-35.5	-34.7	-31.7	-29.0	-23.8	-18.6	-17.5	-
HKG, SFO	-	-35.5	-34.6	-33.2	-30.0	-26.8	-24.2	-21.9	-
AKL, SFO	-	-34.8	-33.0	-31.0	-28.4	-27.0	-26.1	-25.2	-
LAX, HND(NRT)	-37.2	-35.4	-34.2	-31.9	-29.0	-26.2	-24.1	-22.8	-18.4

Route	Probability	<u>Average Temperature, °C</u>							
		1%	5%	10%	25%	50%	75%	90%	95%
JFK, BAH	-	-59.9	-58.7	-57.2	-53.8	-52.1	-50.0	-49.1	-
GIG, JFK	-	-58.8	-57.5	-55.8	-53.5	-48.2	-41.5	-39.8	-
HKG, SFO	-	-55.8	-54.6	-53.8	-50.8	-48.8	-47.5	-45.2	-
AKL, SFO	-	-56.3	-55.3	-54.3	-52.4	-50.4	-49.2	-49.0	-
LAX, HND(NRT)	-60.9	-58.9	-57.9	-56.1	-53.5	-51.4	-49.8	-47.2	-46.1



(a) Winter



(b) Summer

Figure 1. Vertical cross-sections of the meridional distribution of temperatures (adapted from ref. 4, fig. 4.1).

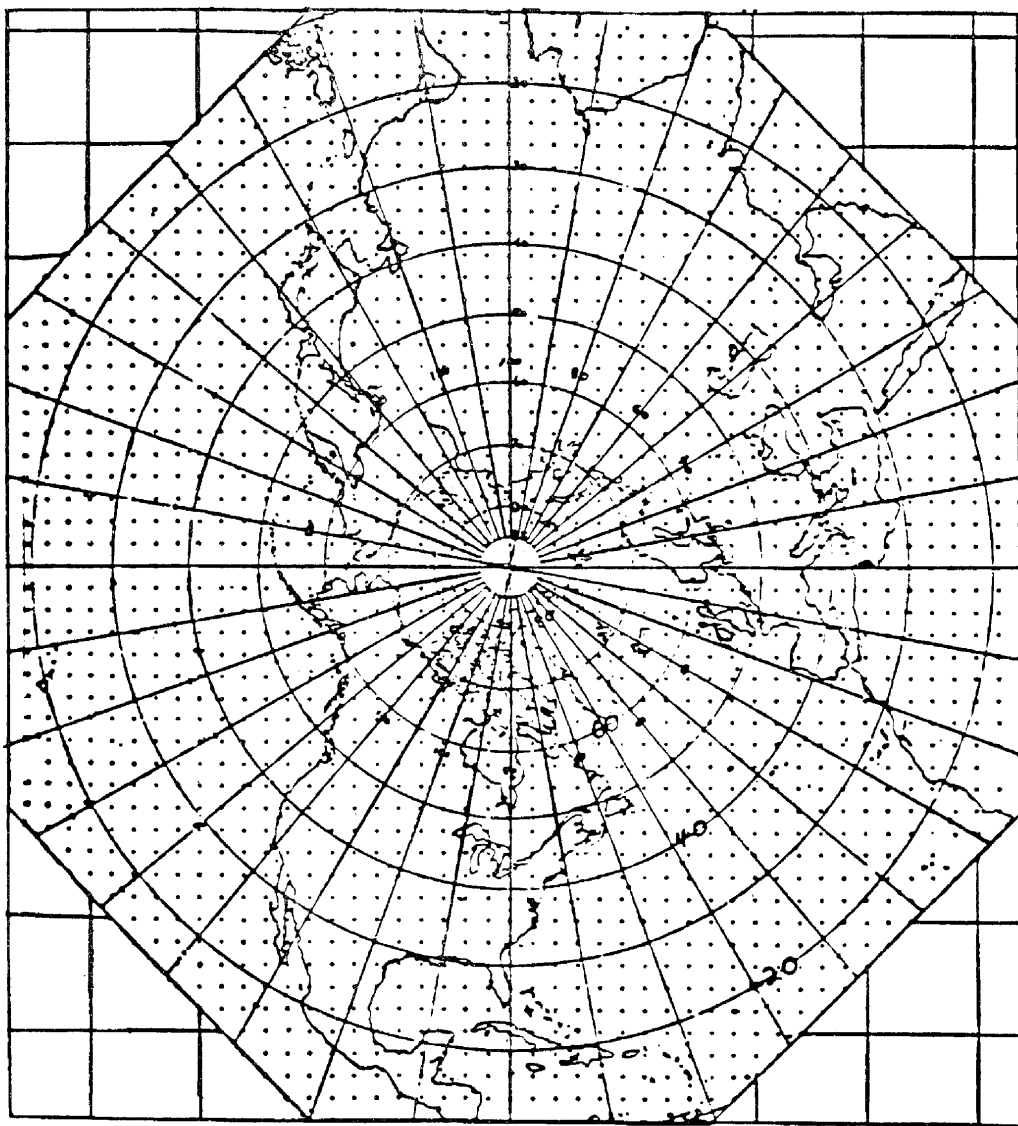


Figure 2. Grid points for National Meteorological Center (NMC) and Global Weather Central (GWC) analysis fields.

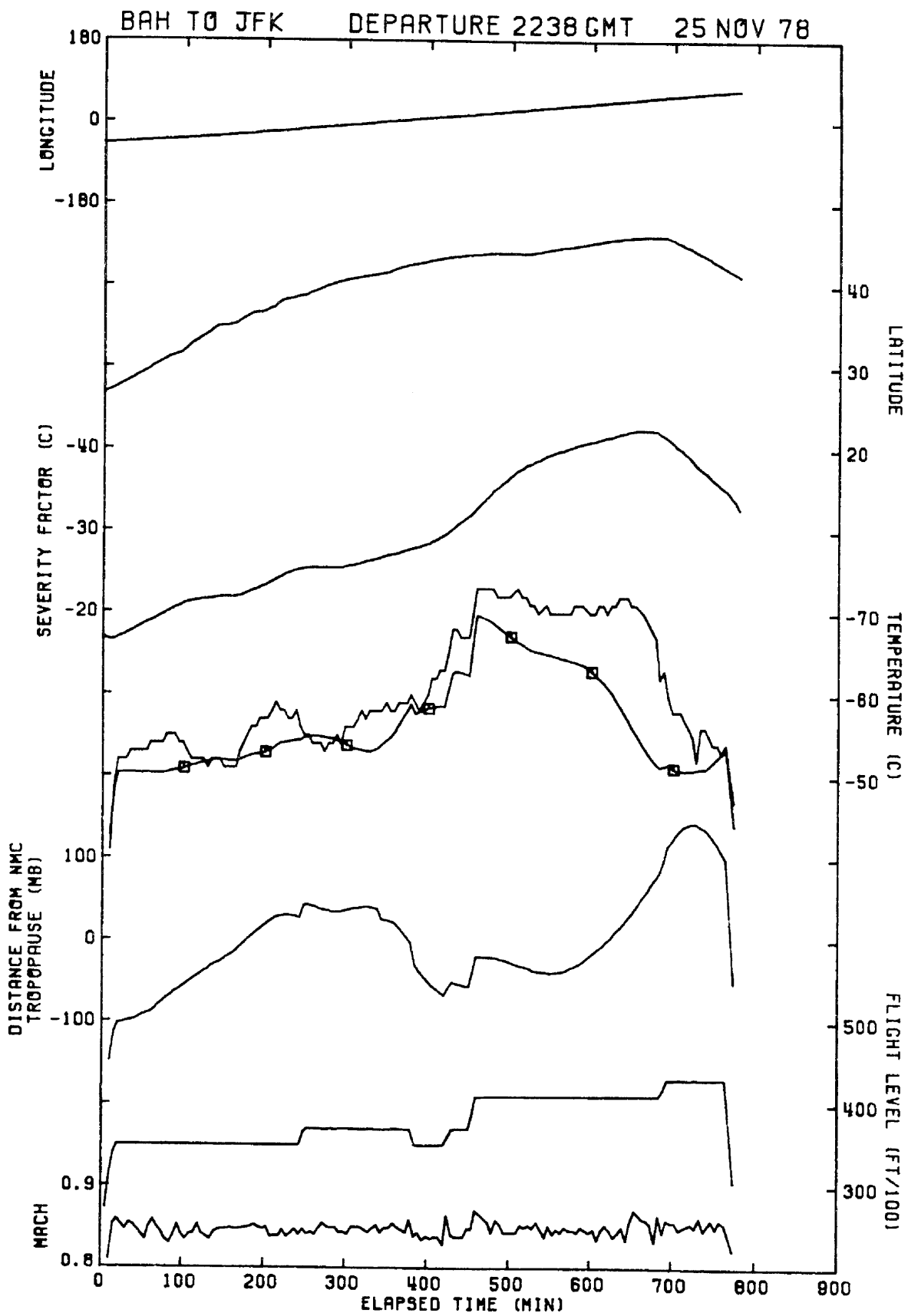


Figure 3. Flight history for flight rank 1.

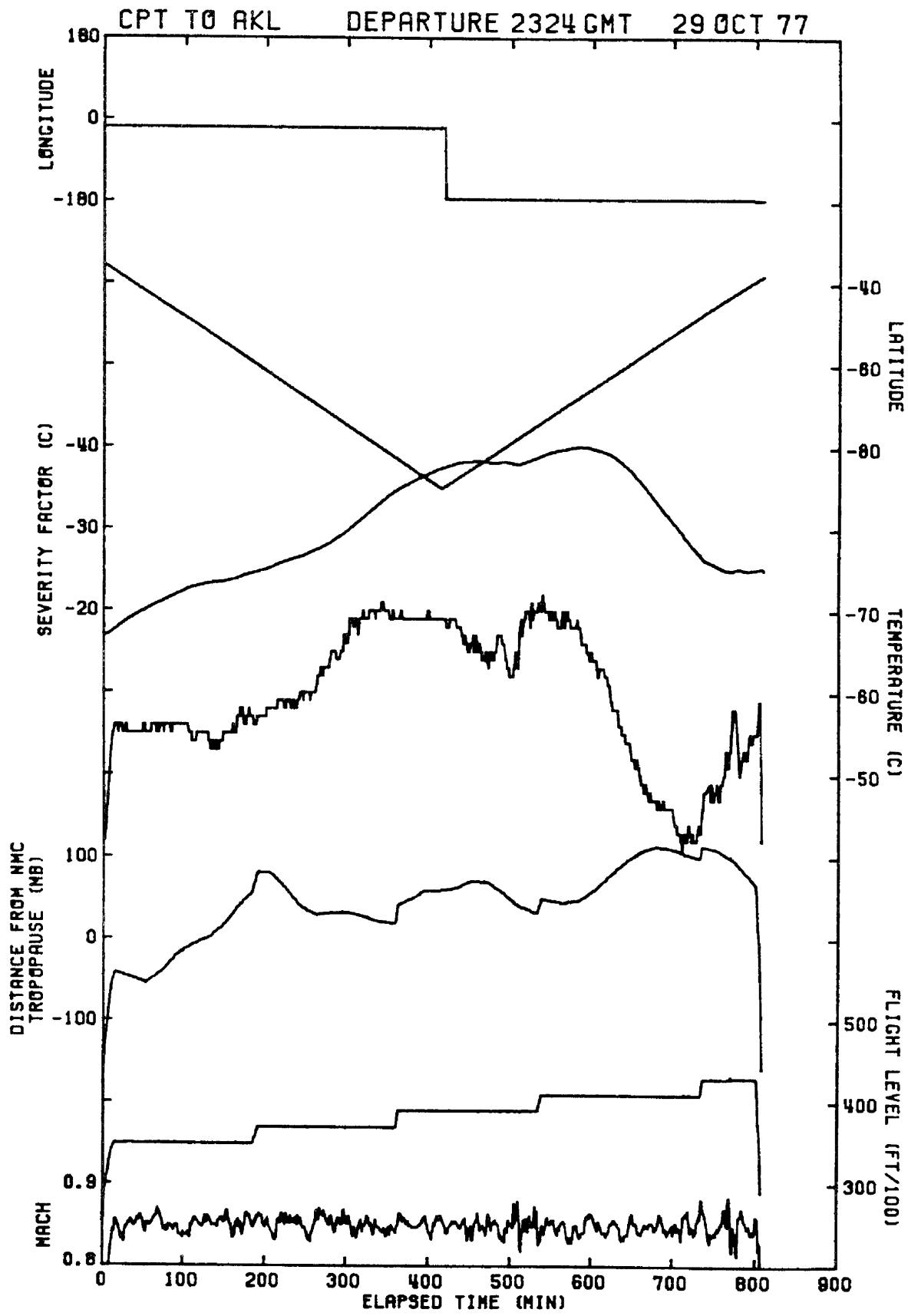


Figure 4. Flight history for flight rank 2.

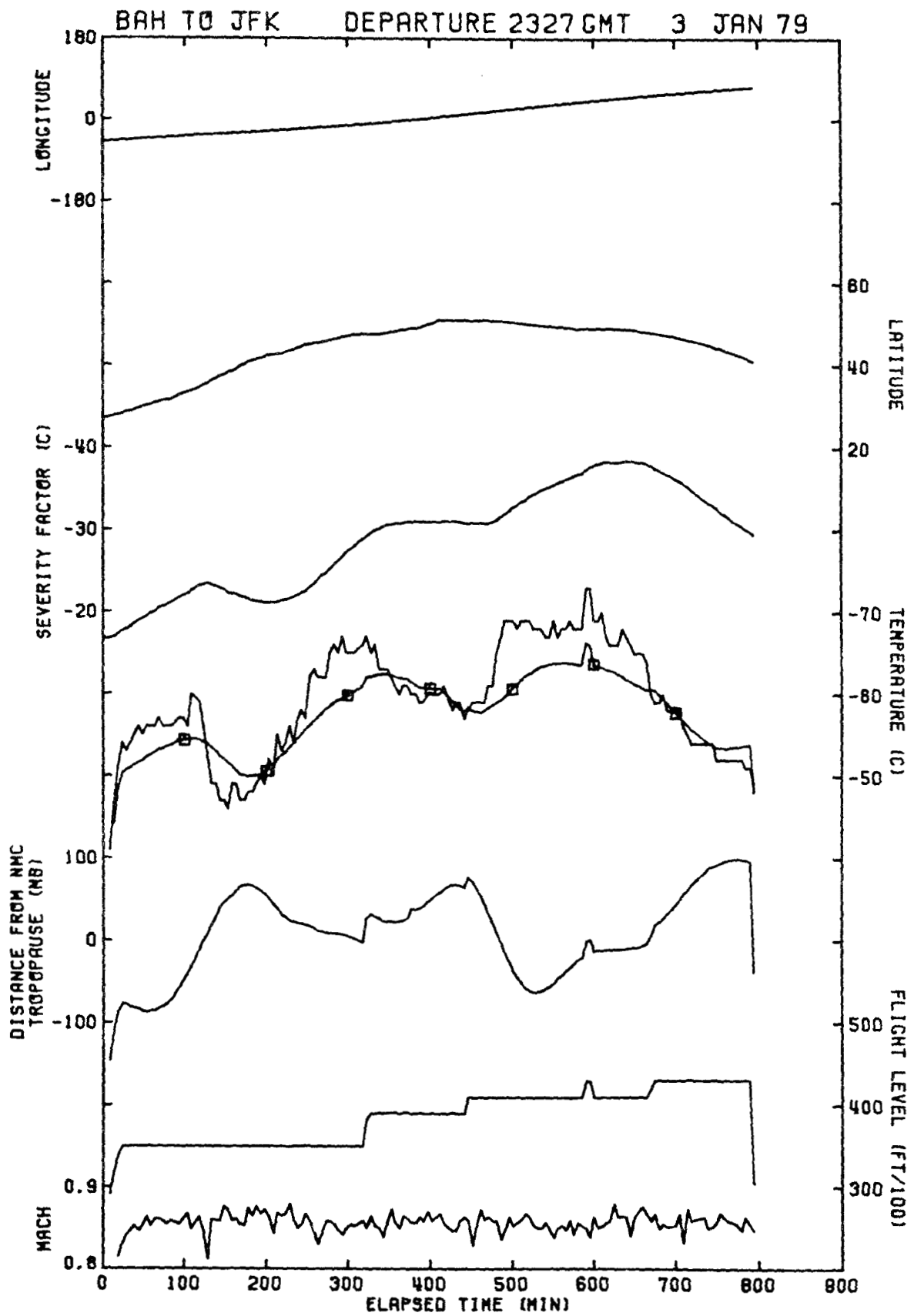


Figure 5. Flight history for flight rank 3.

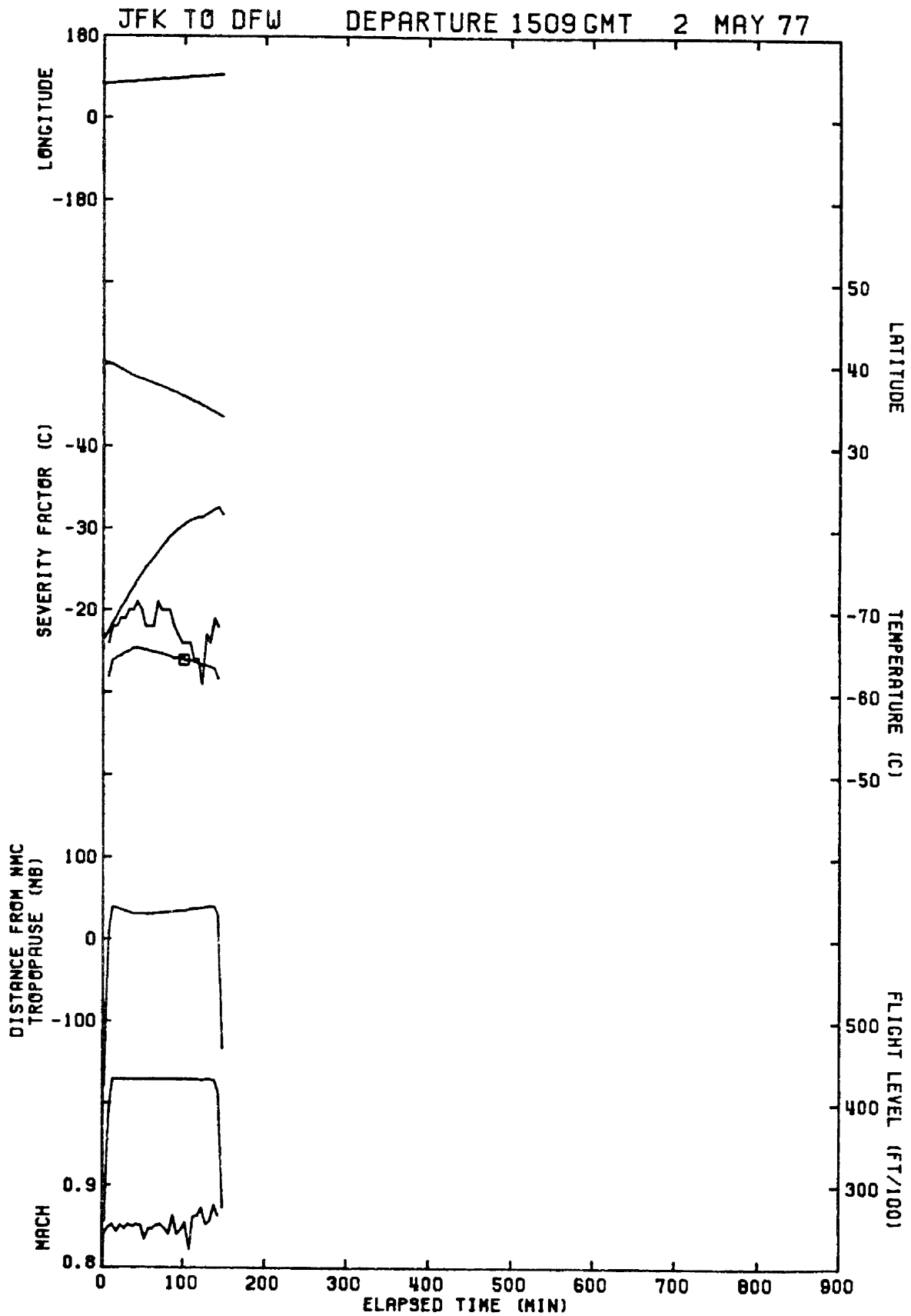


Figure 6. Flight history for flight rank 4.

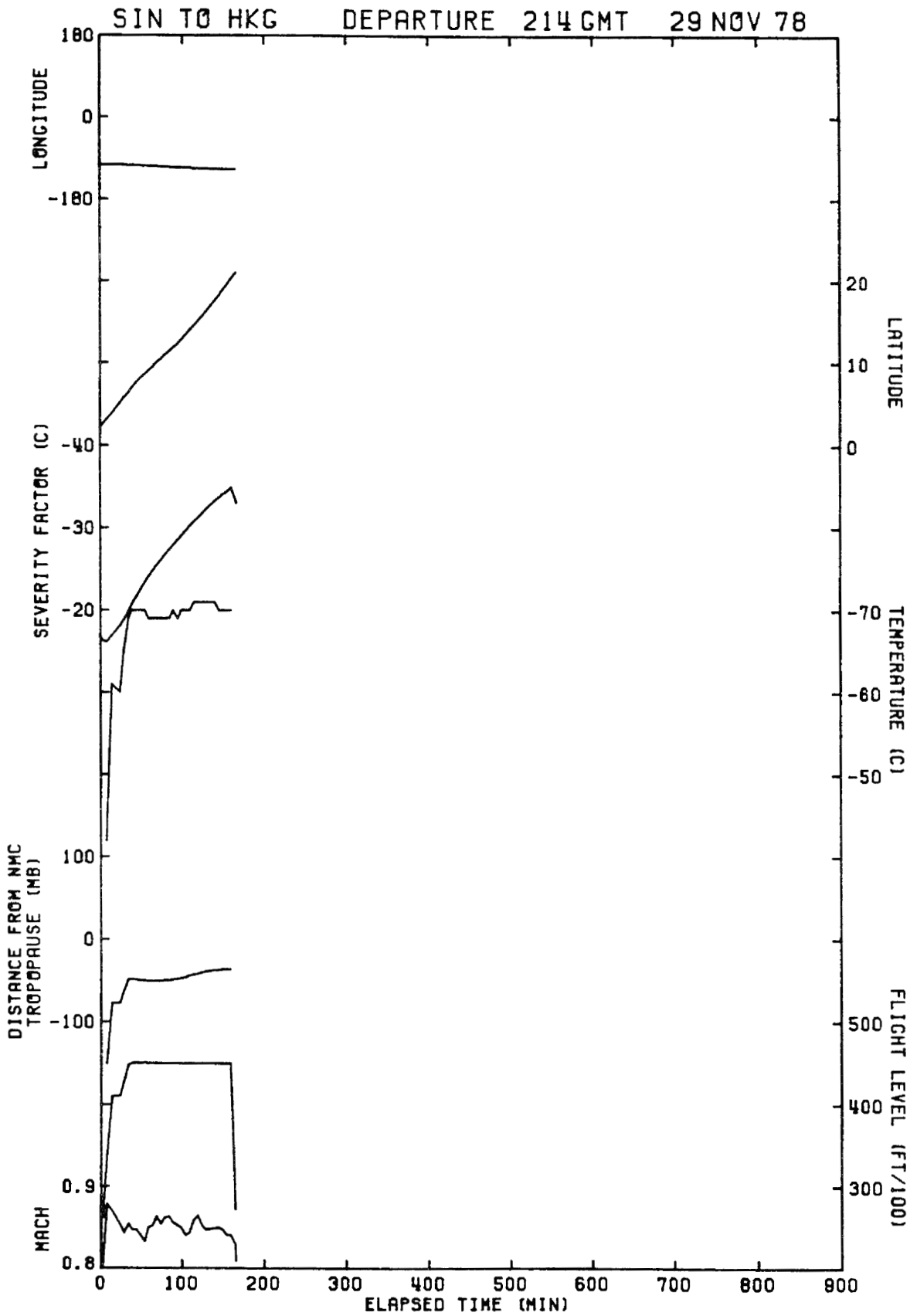


Figure 7. Flight history for flight rank 5.

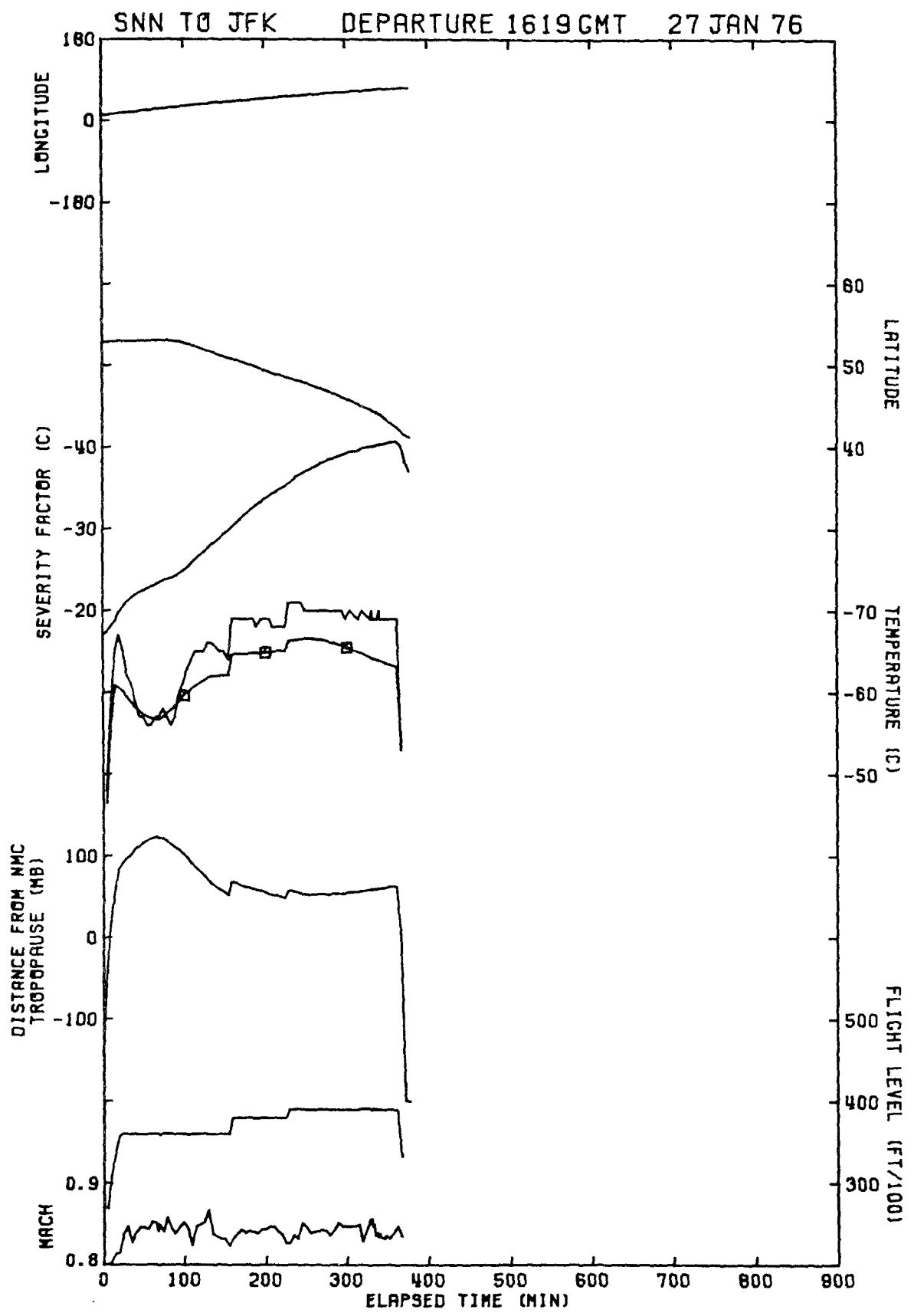


Figure 8. Flight history for flight rank 6.

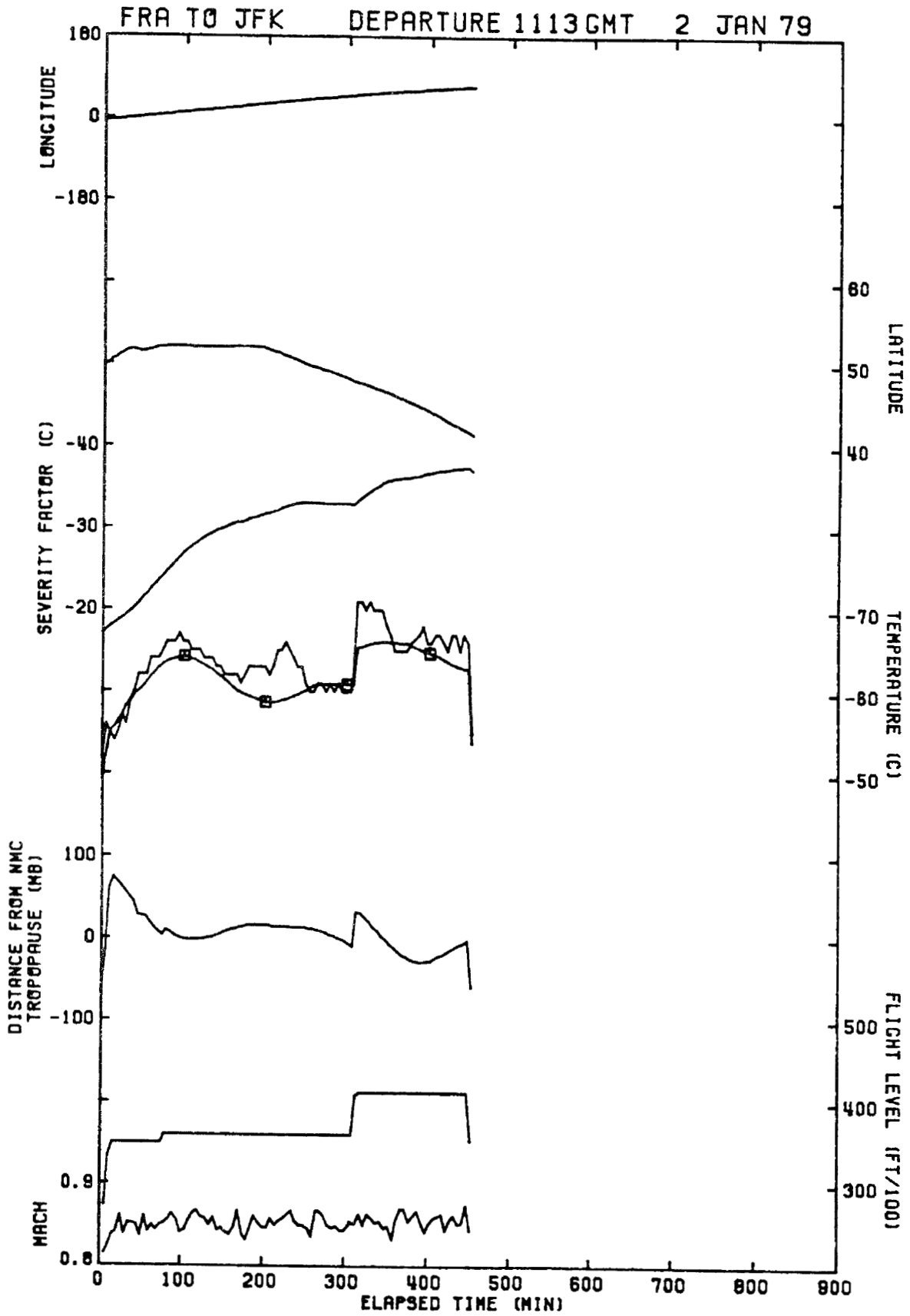


Figure 9. Flight history for flight rank 7.

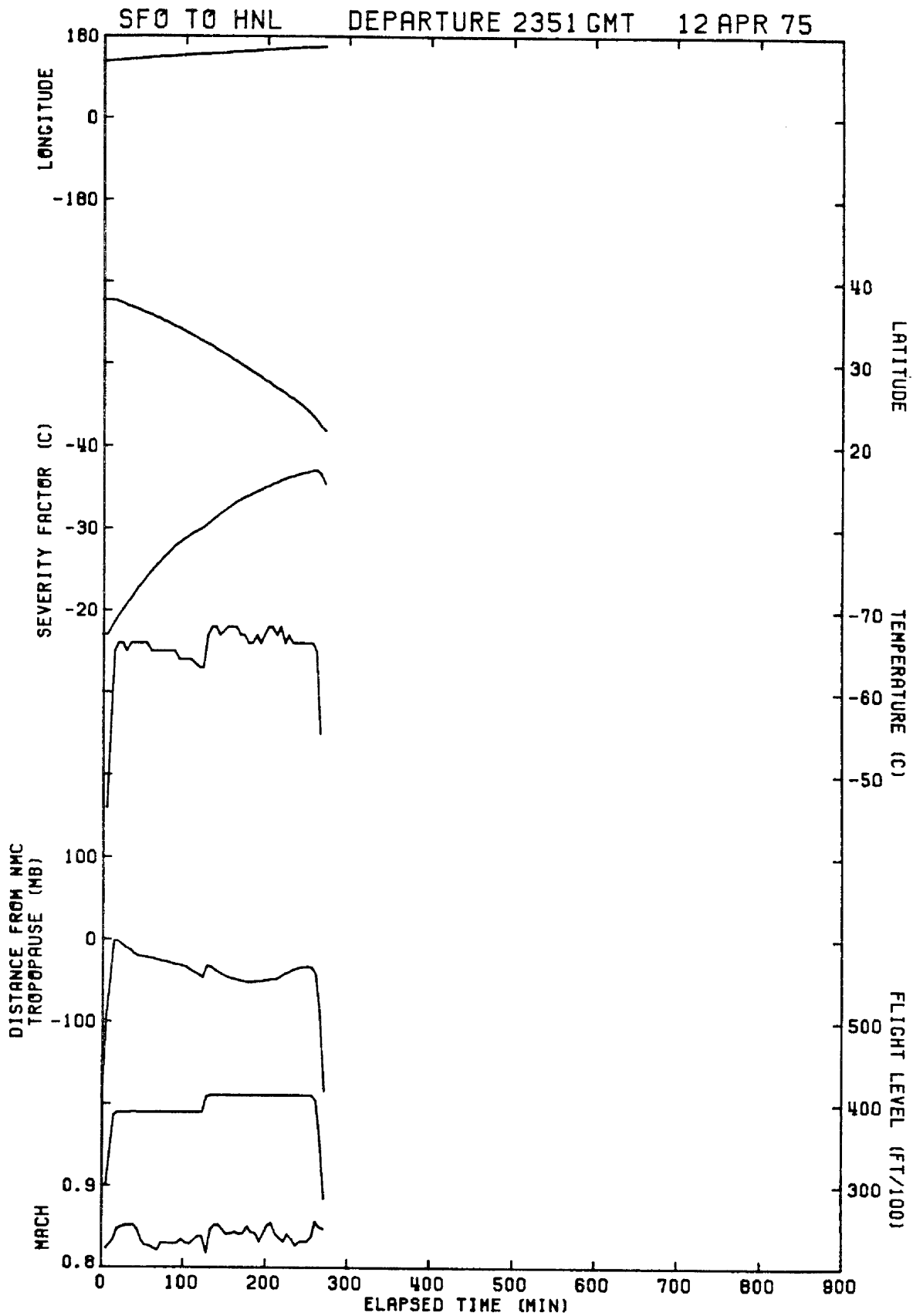


Figure 10. Flight history for flight rank 8.

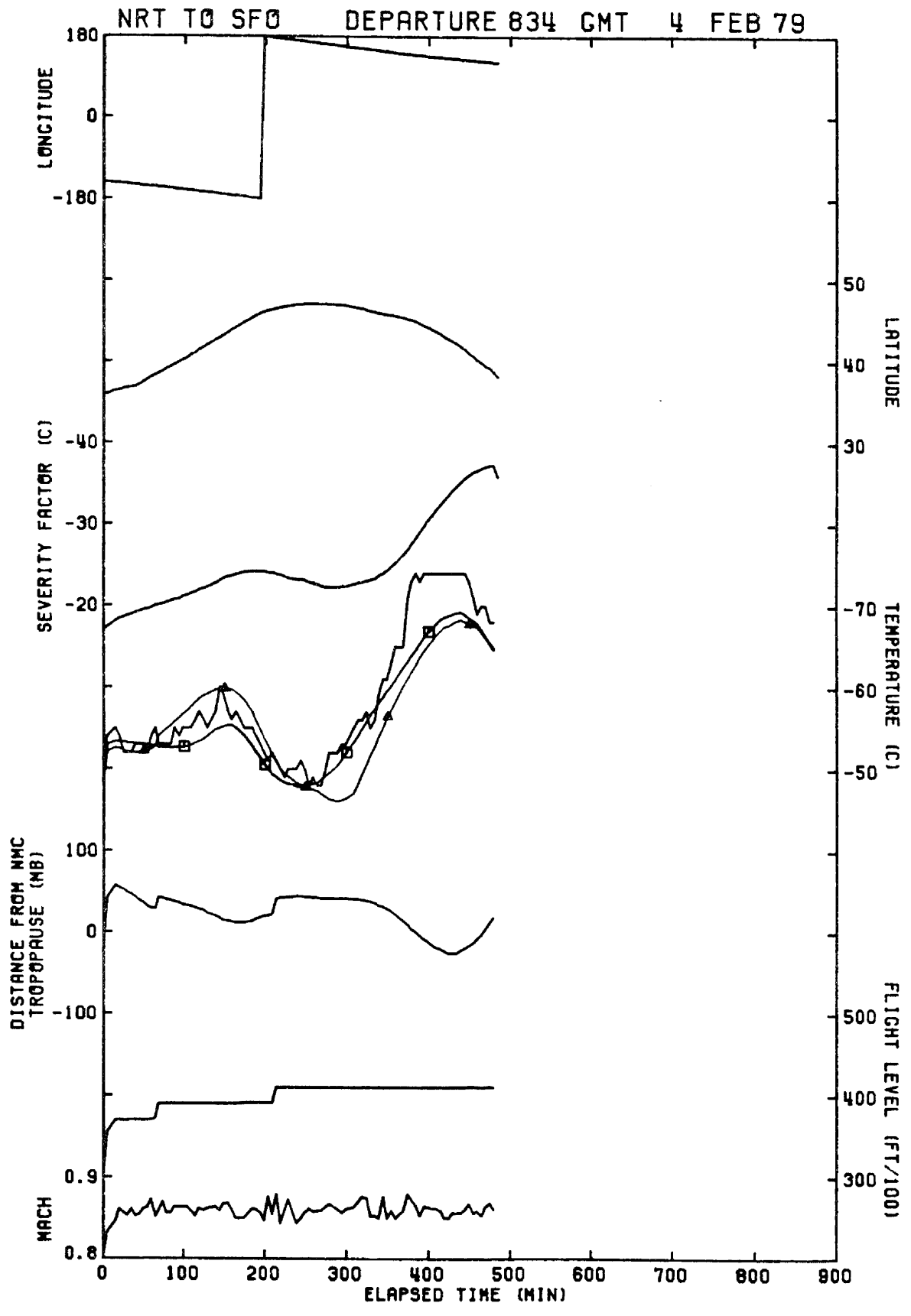


Figure 11. Flight history for flight rank 9.

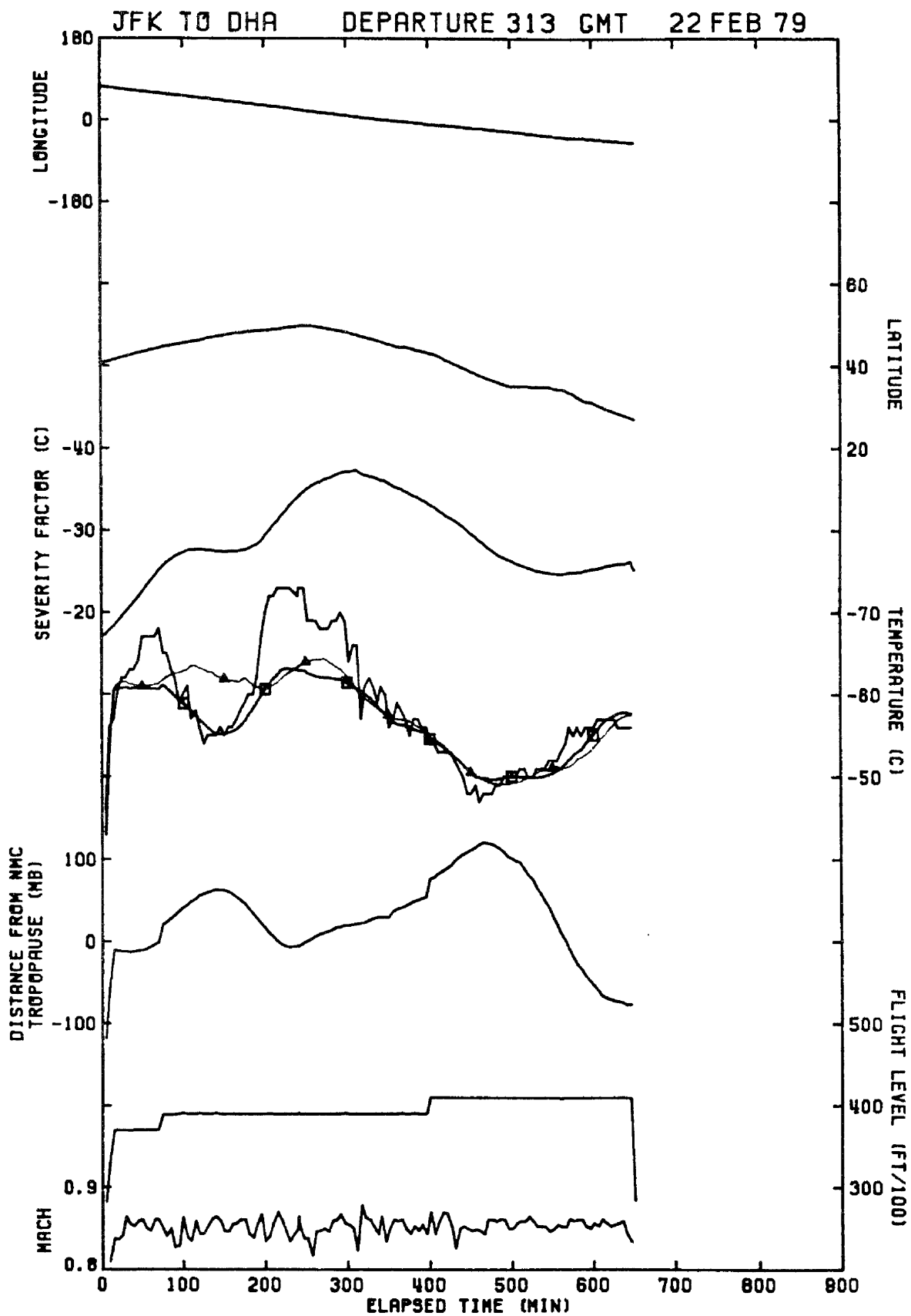


Figure 12. Flight history for flight rank 10.

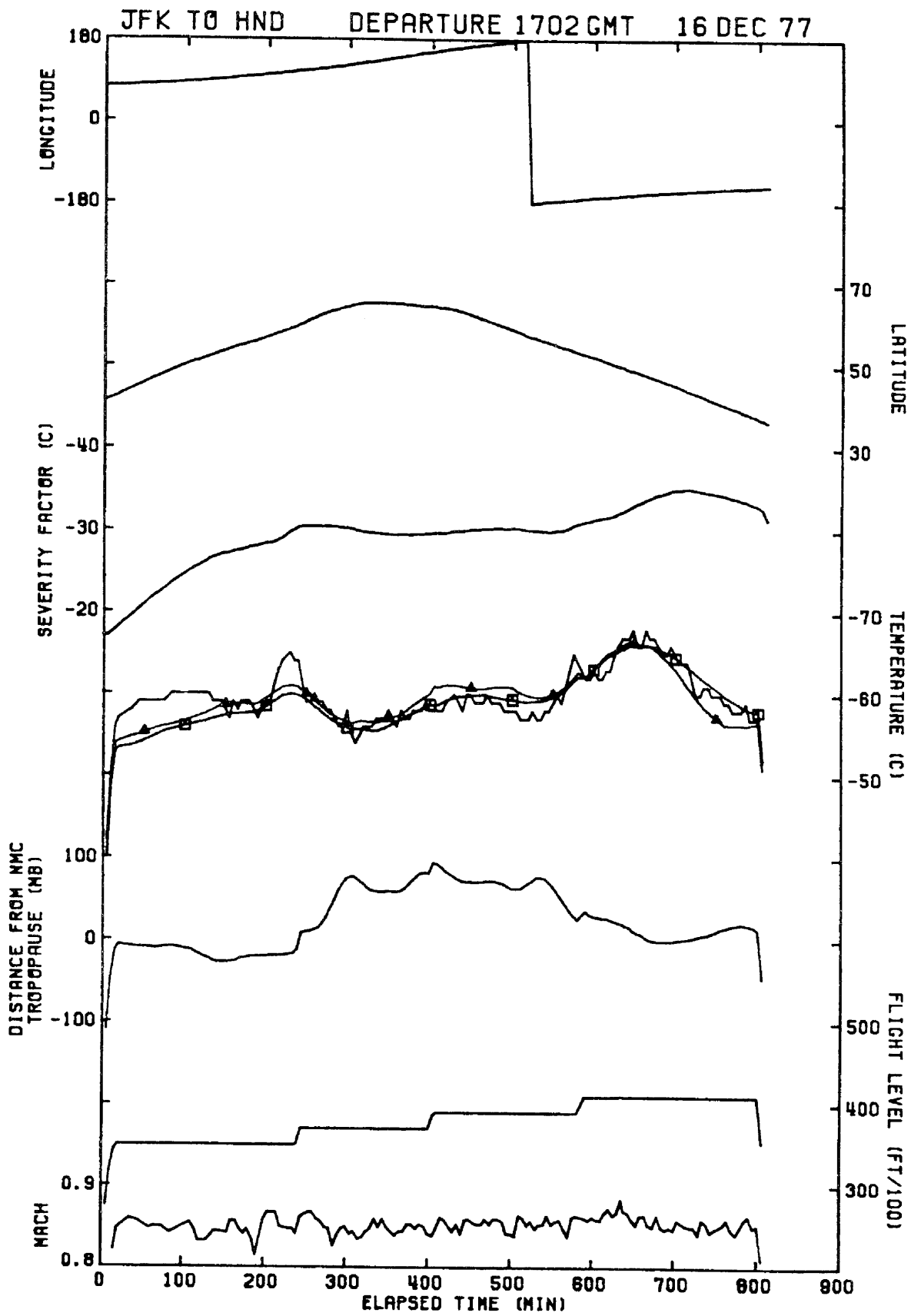


Figure 13. Flight history for flight rank 11.

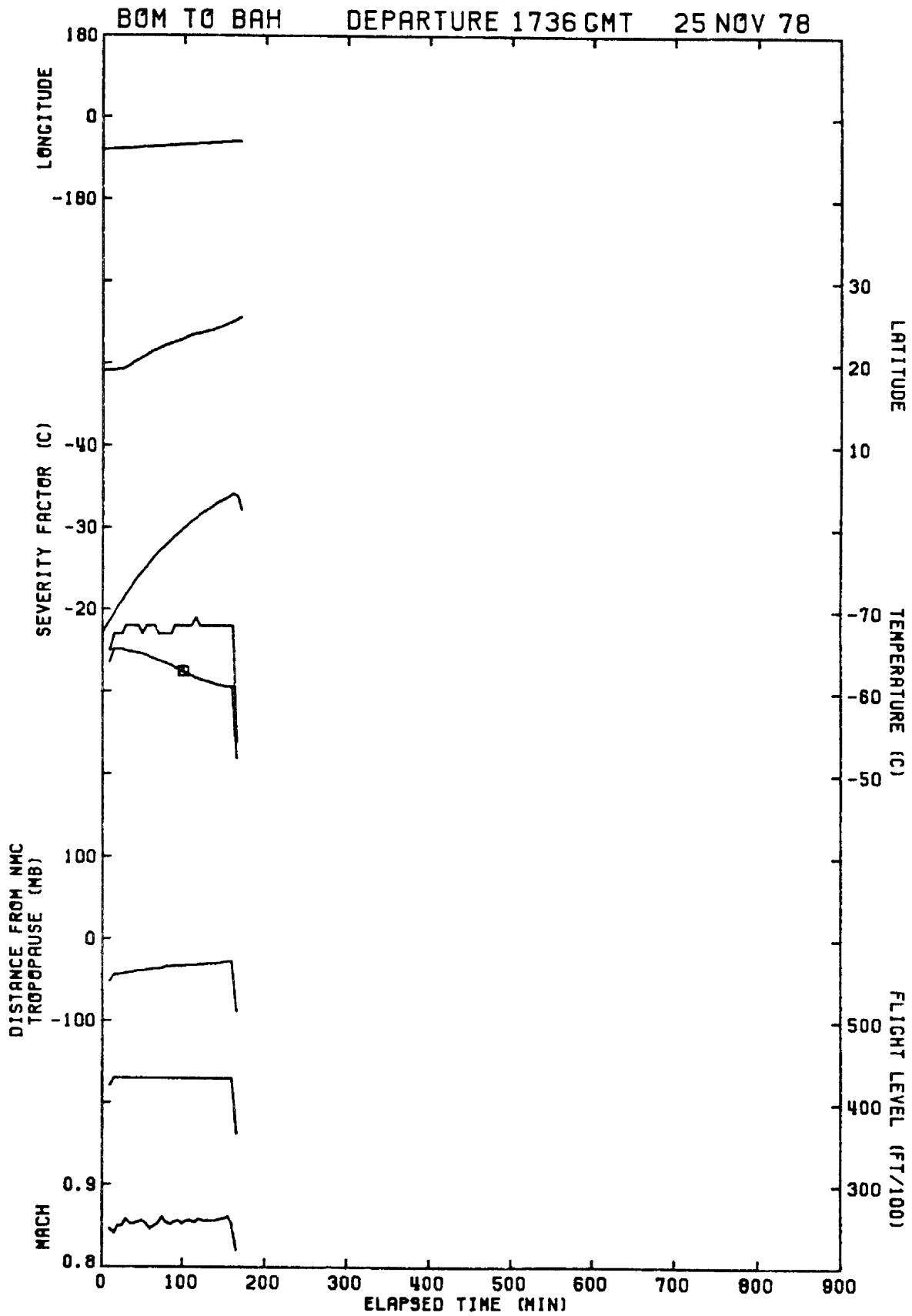


Figure 14. Flight history for flight rank 12.

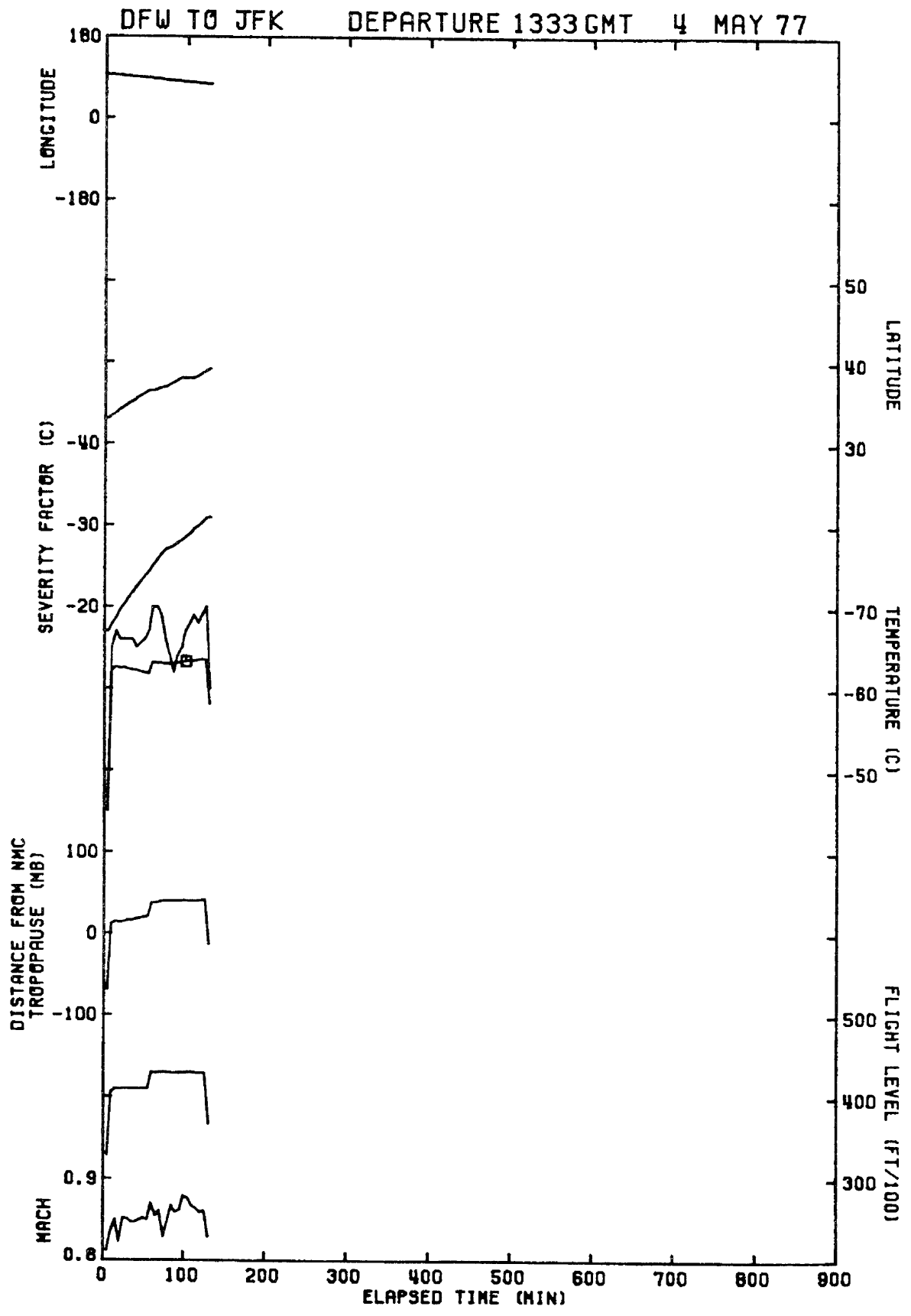


Figure 15. Flight history for flight rank 13.

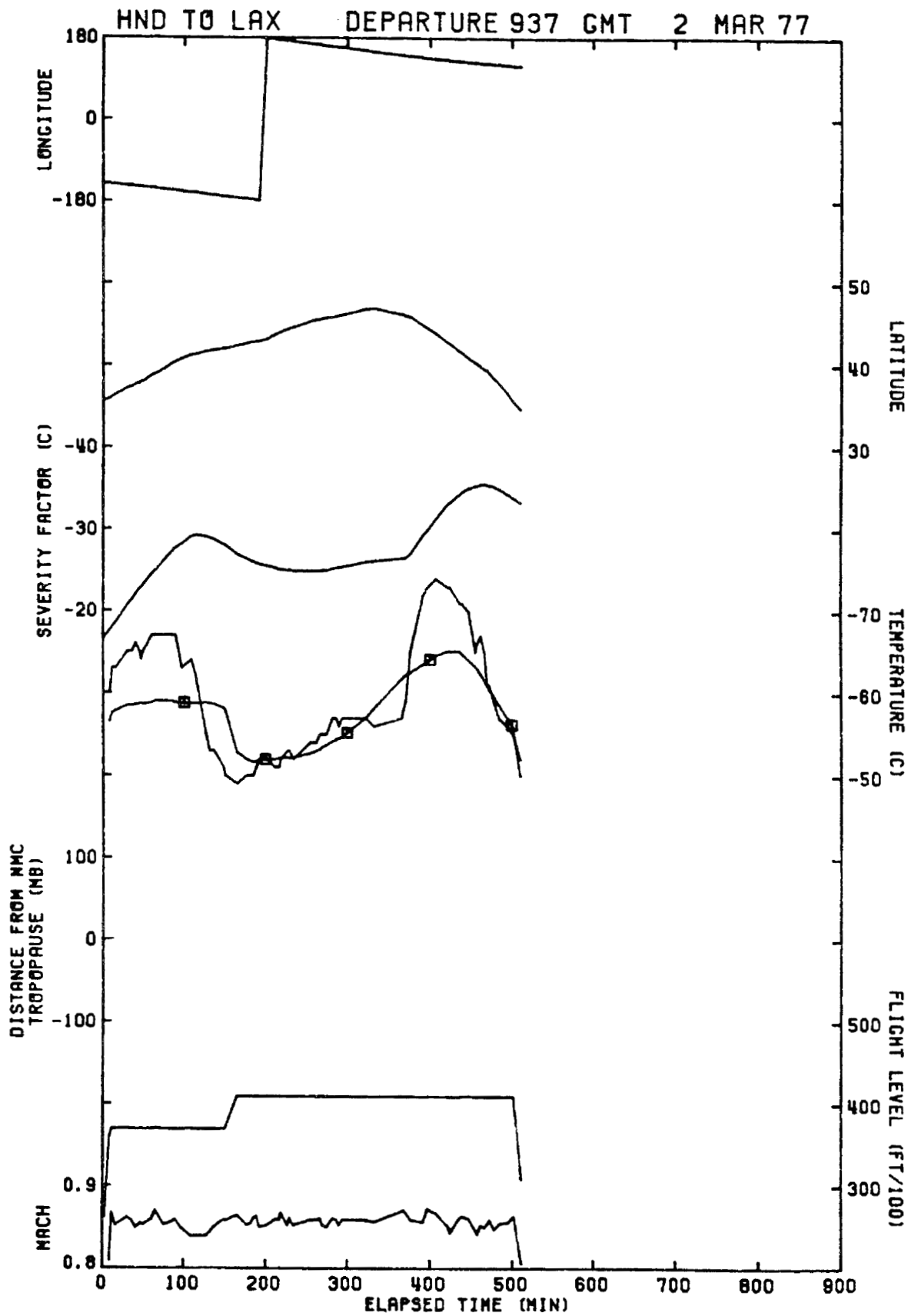


Figure 16. Flight history for flight rank 14.

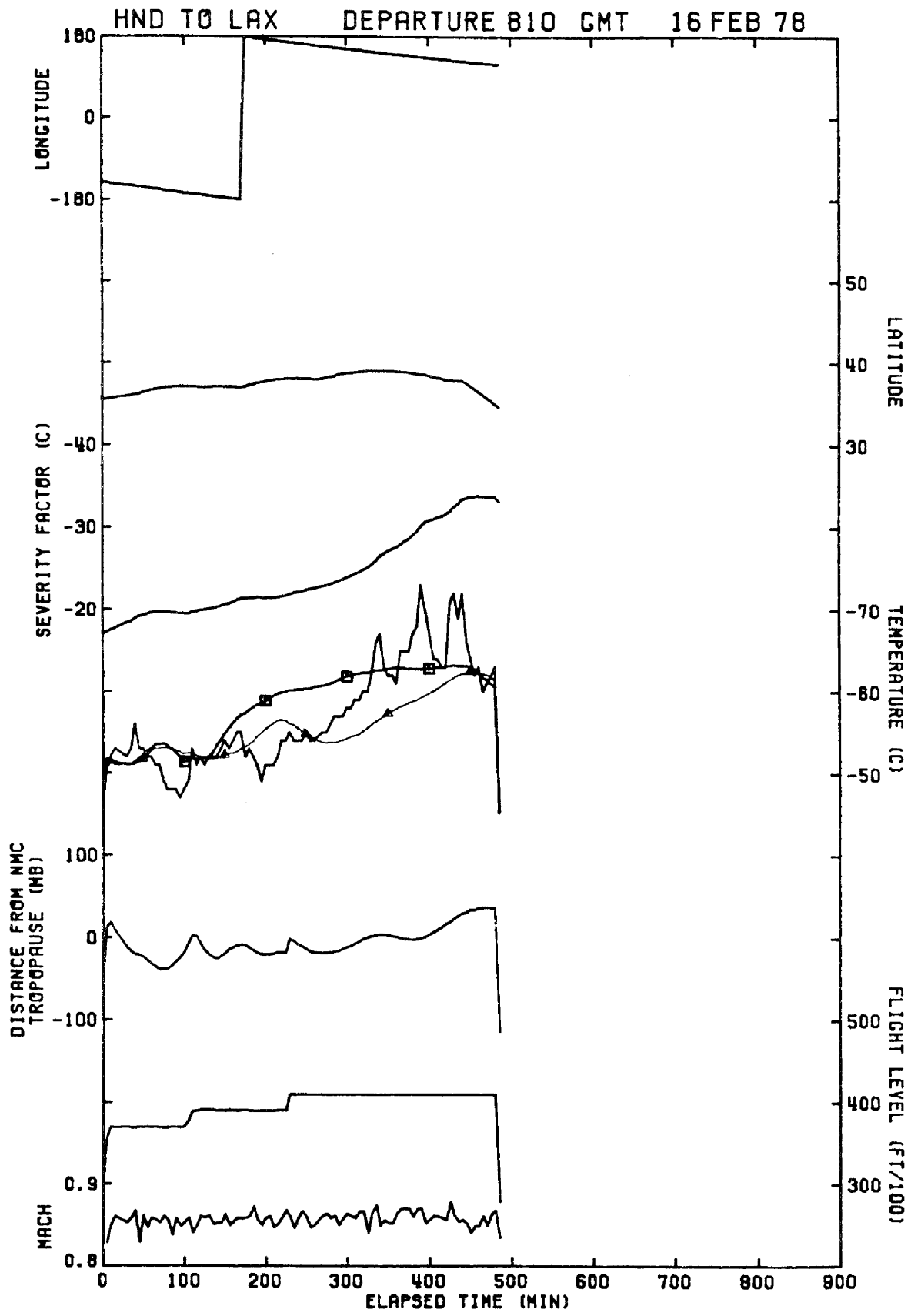


Figure 17. Flight history for flight rank 15.

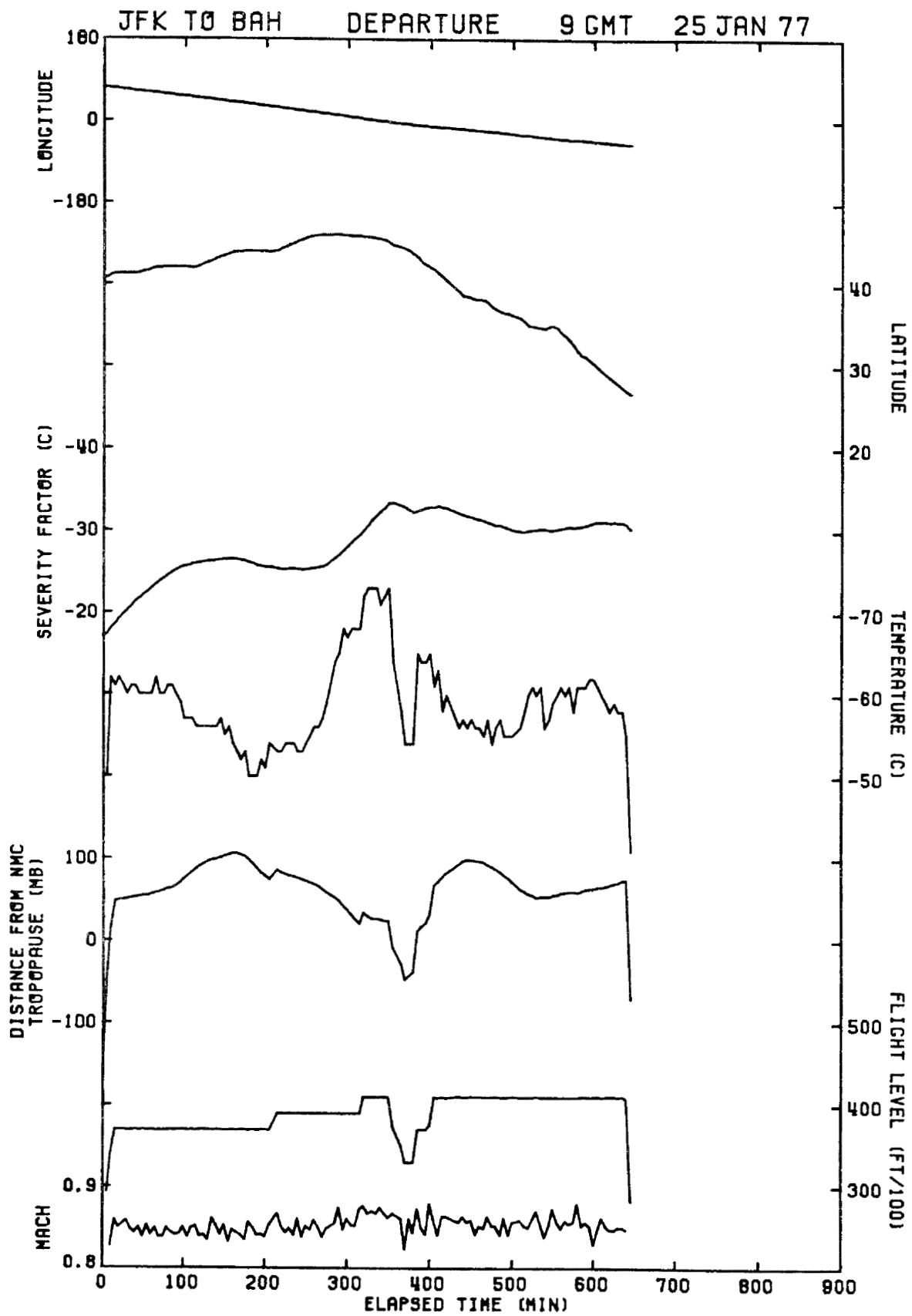


Figure 18. Flight history for flight rank 16.

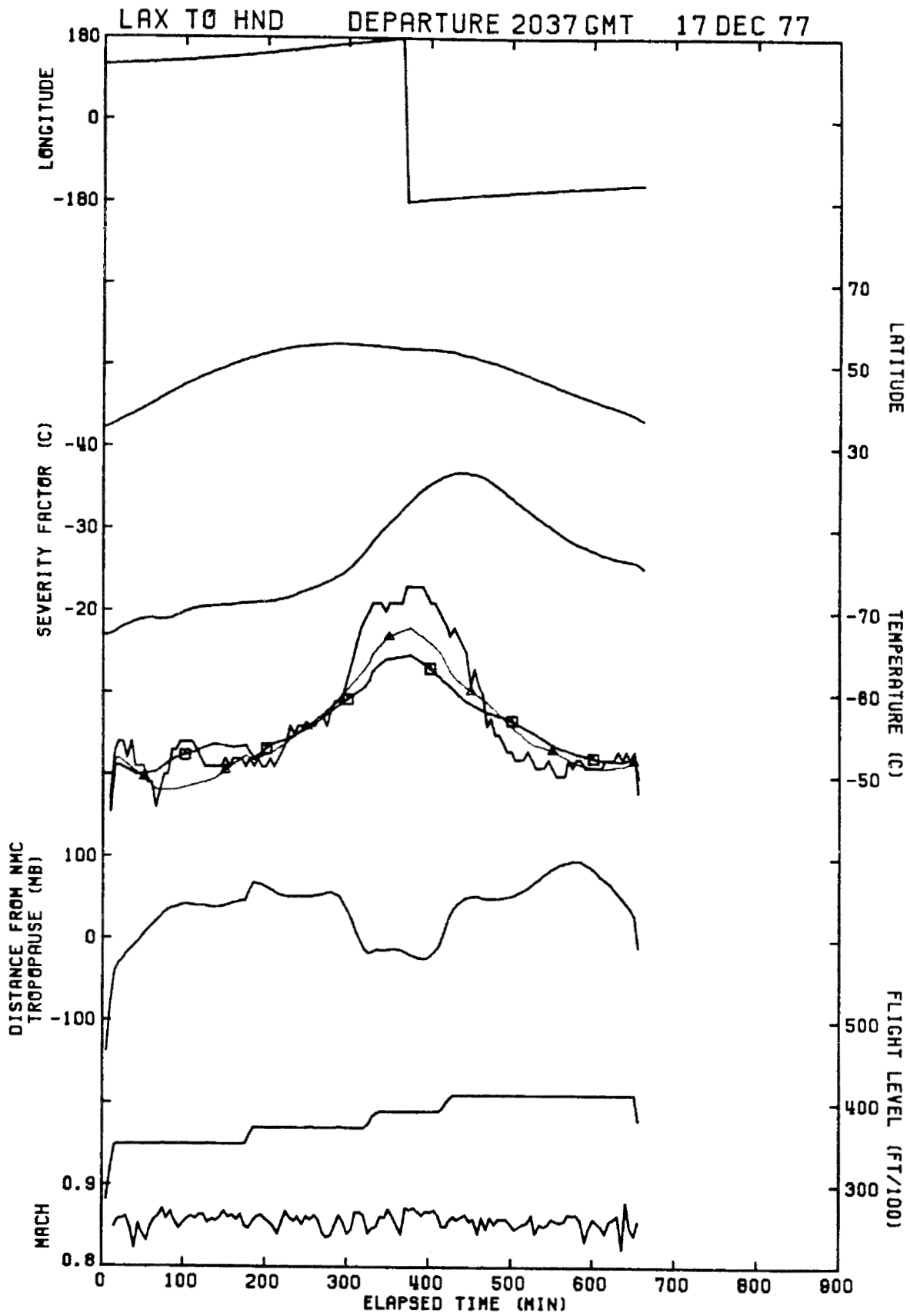


Figure 19. Flight history for flight rank 17.

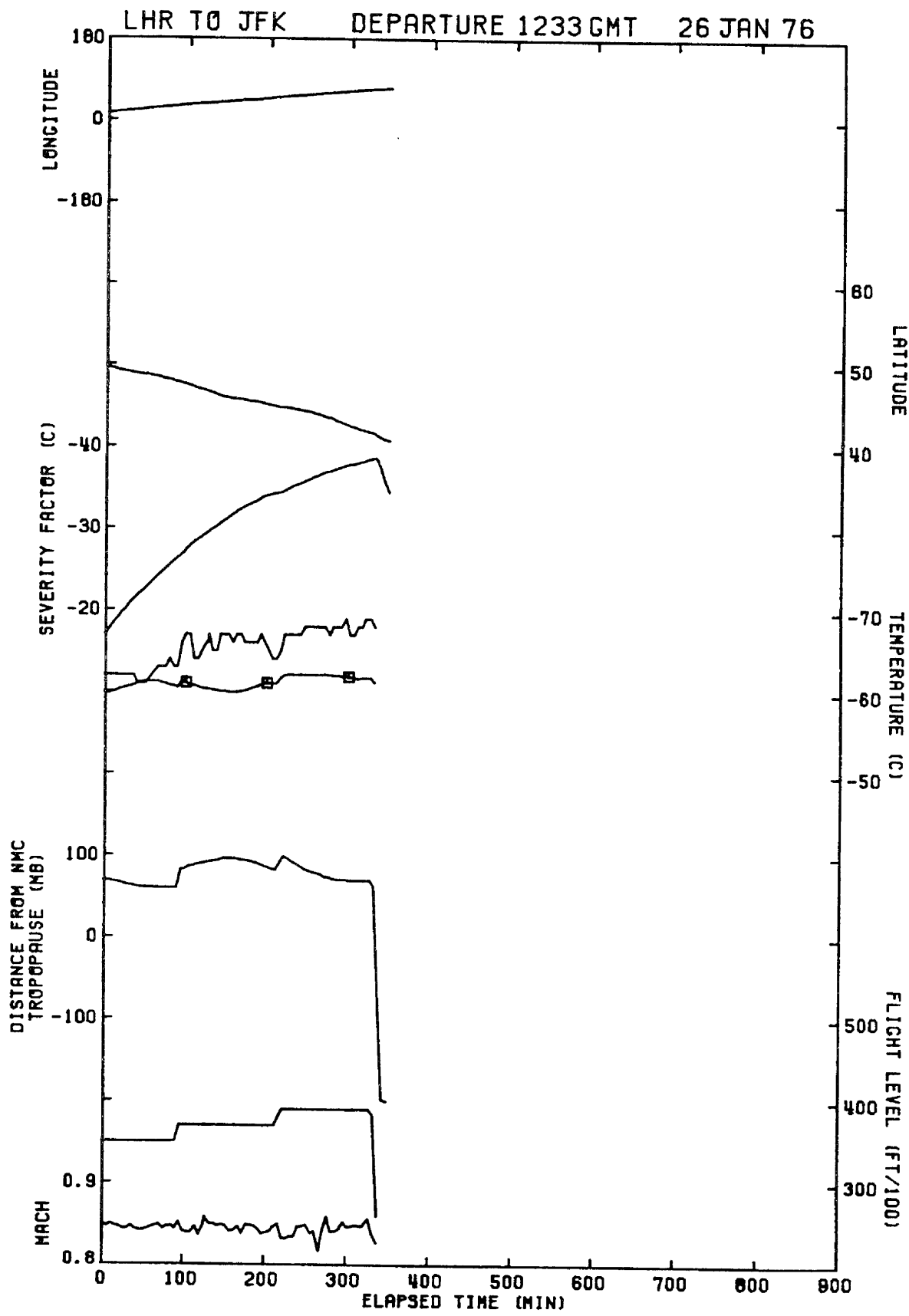


Figure 20. Flight history for flight rank 18.

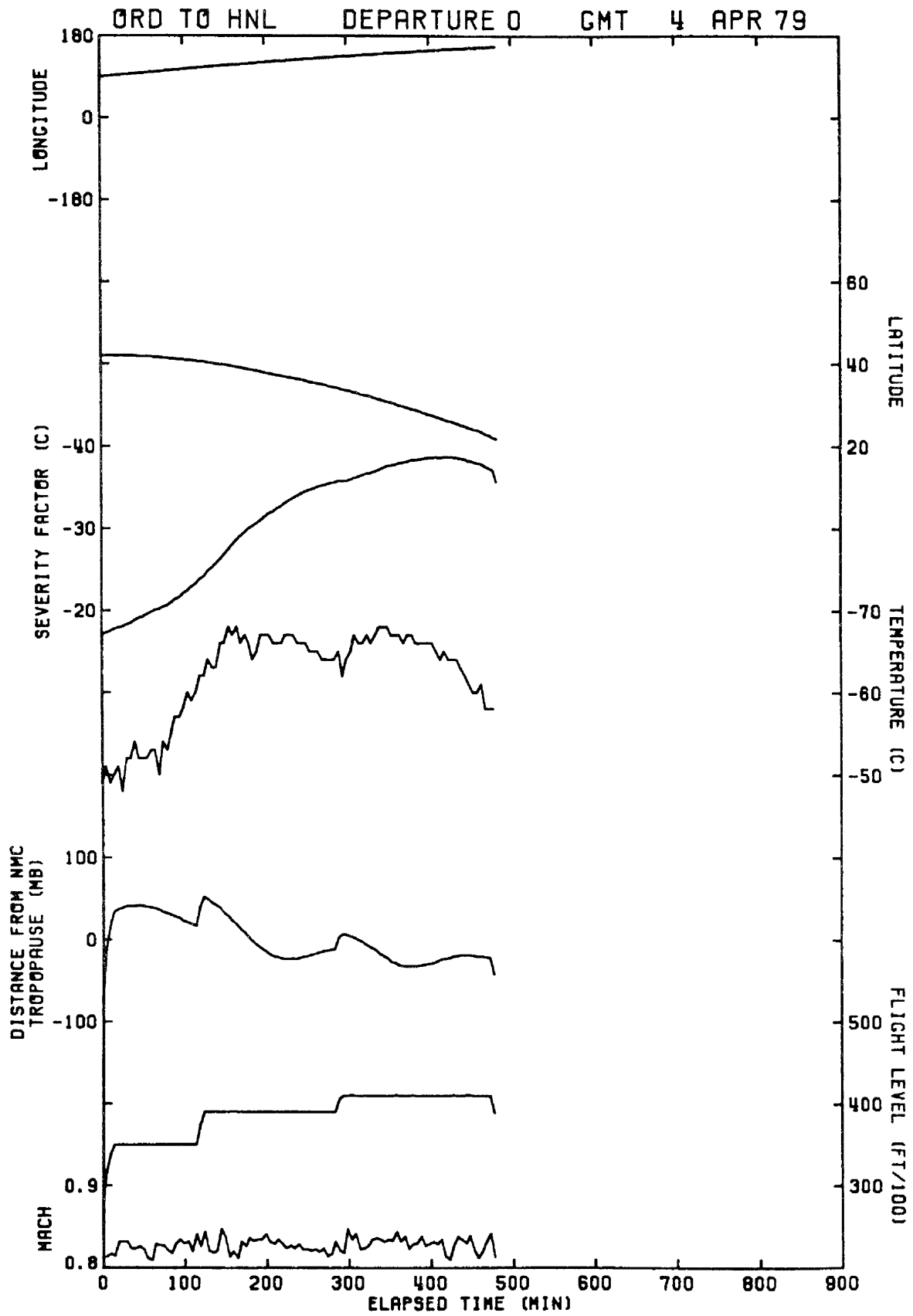


Figure 21. Flight history for flight rank 19.

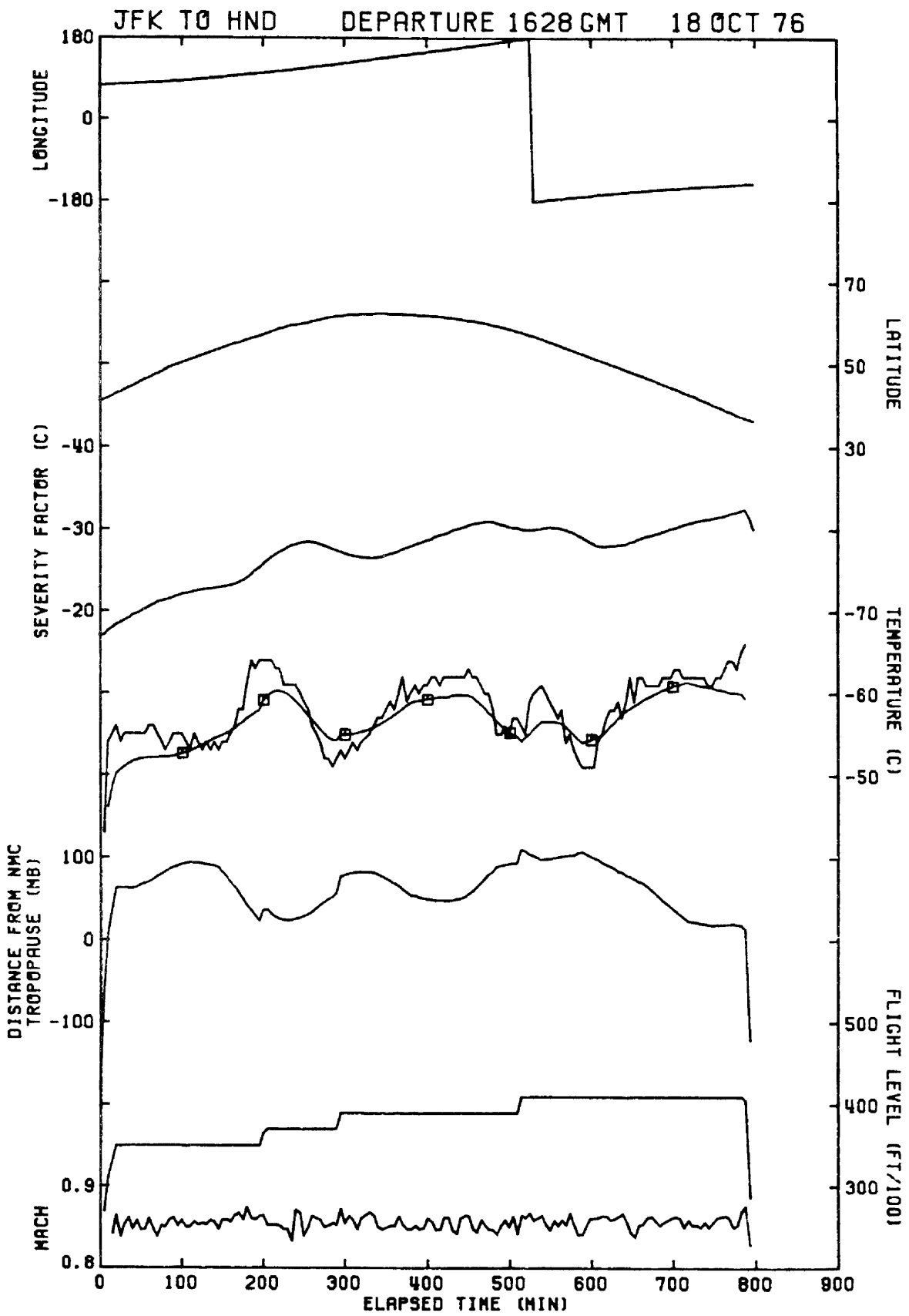


Figure 22. Flight history for flight rank 20.

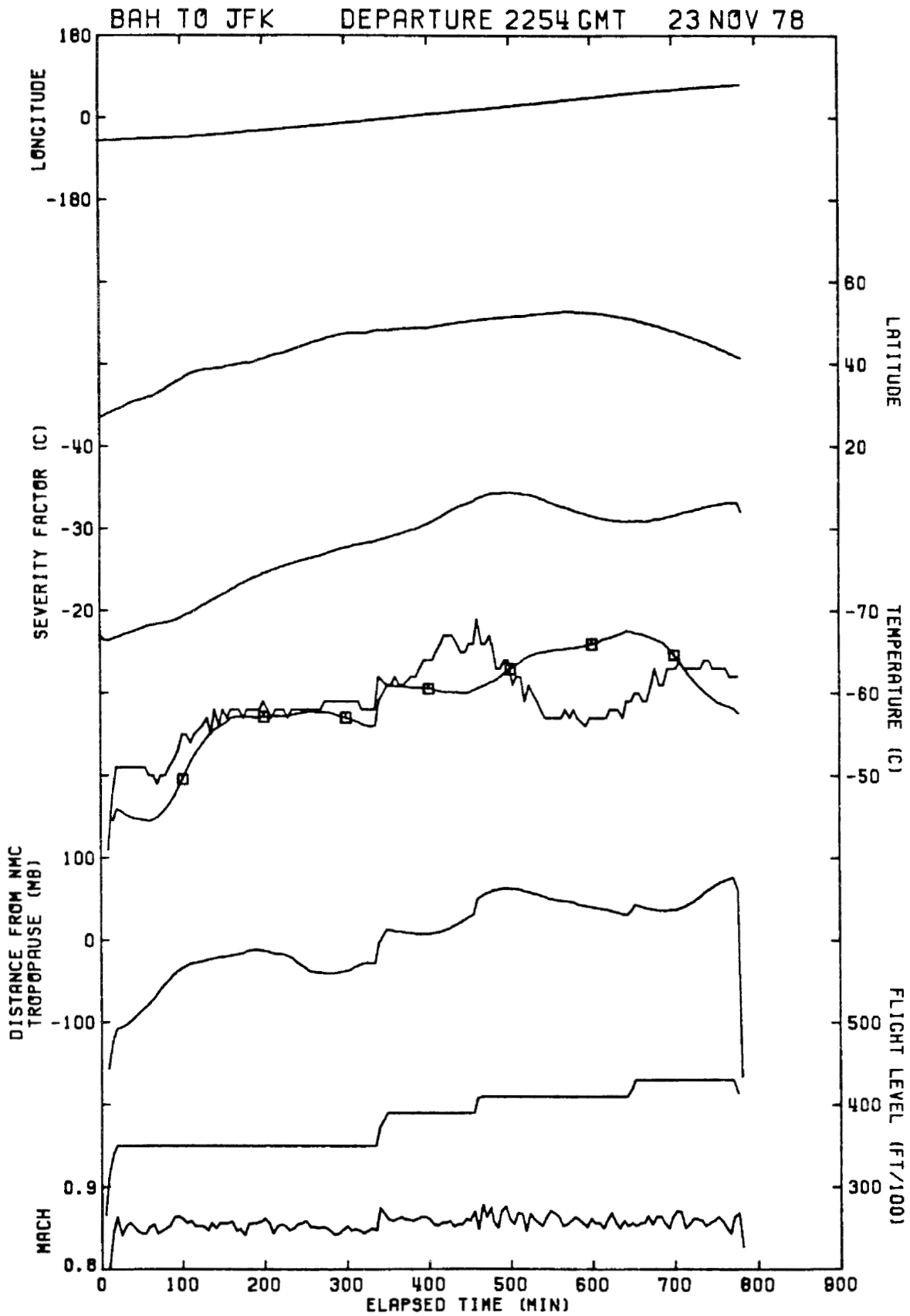


Figure 23. Flight history for flight rank 21.

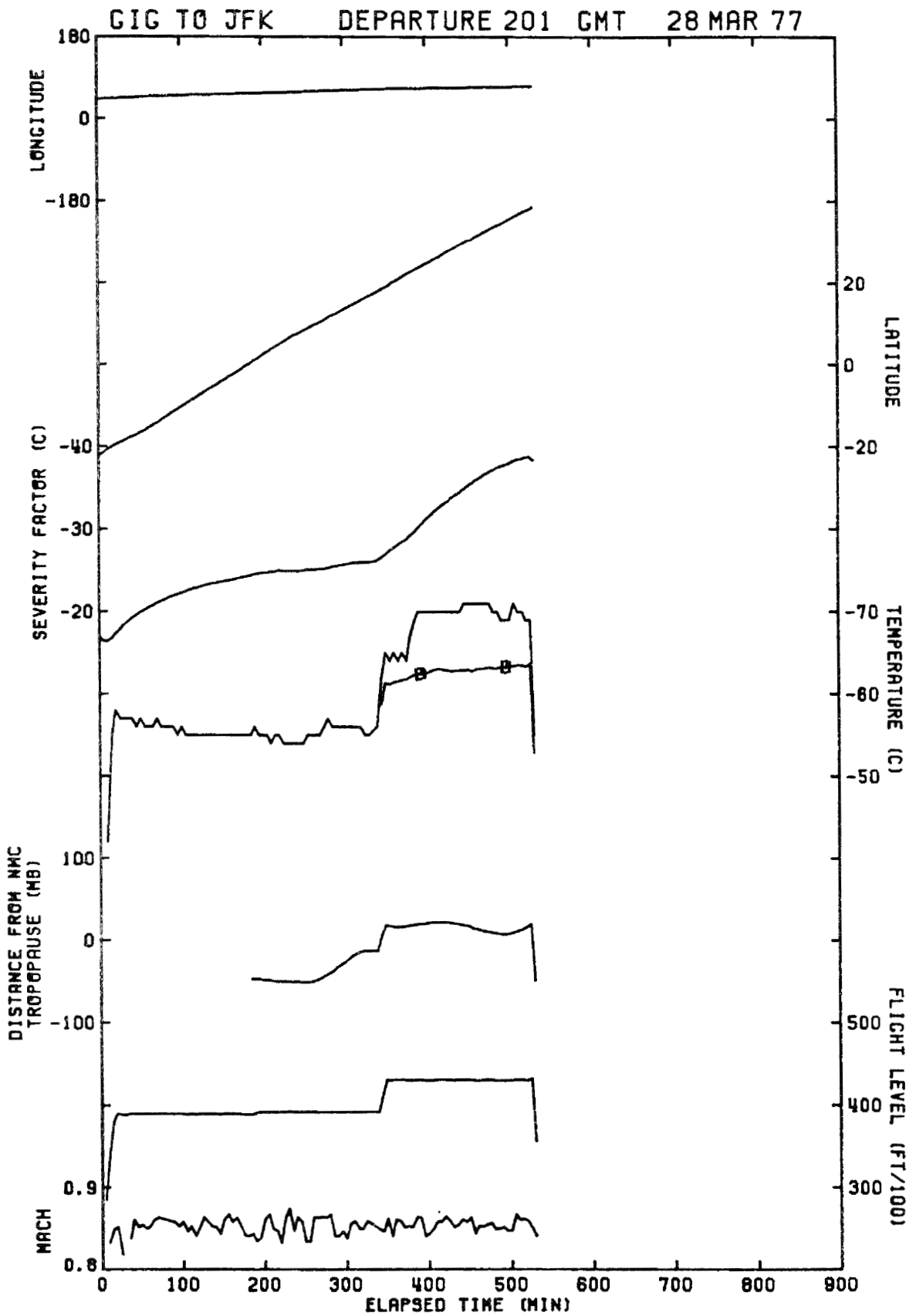


Figure 24. Flight history for flight rank 22.

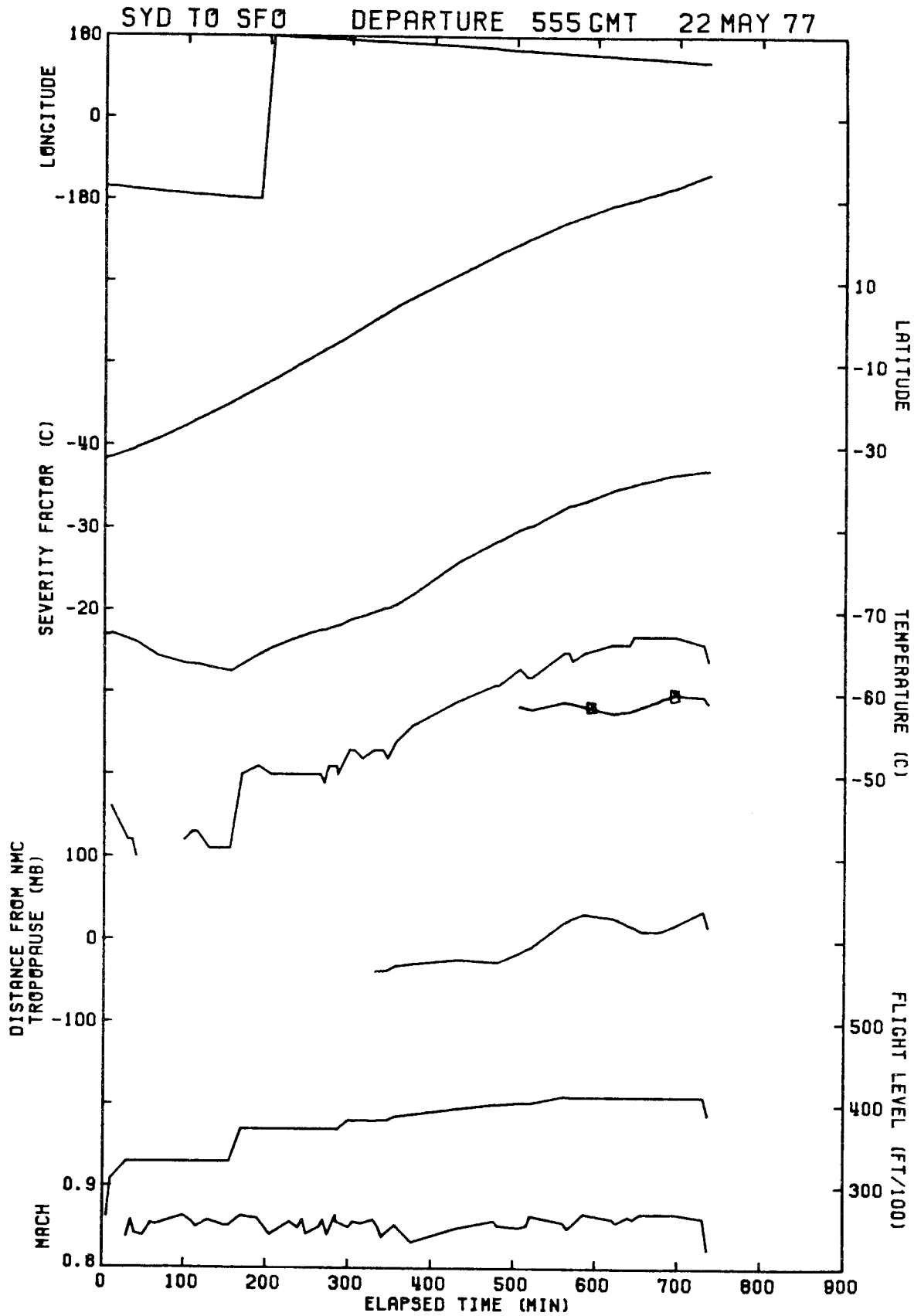


Figure 25. Flight history for flight rank 23.

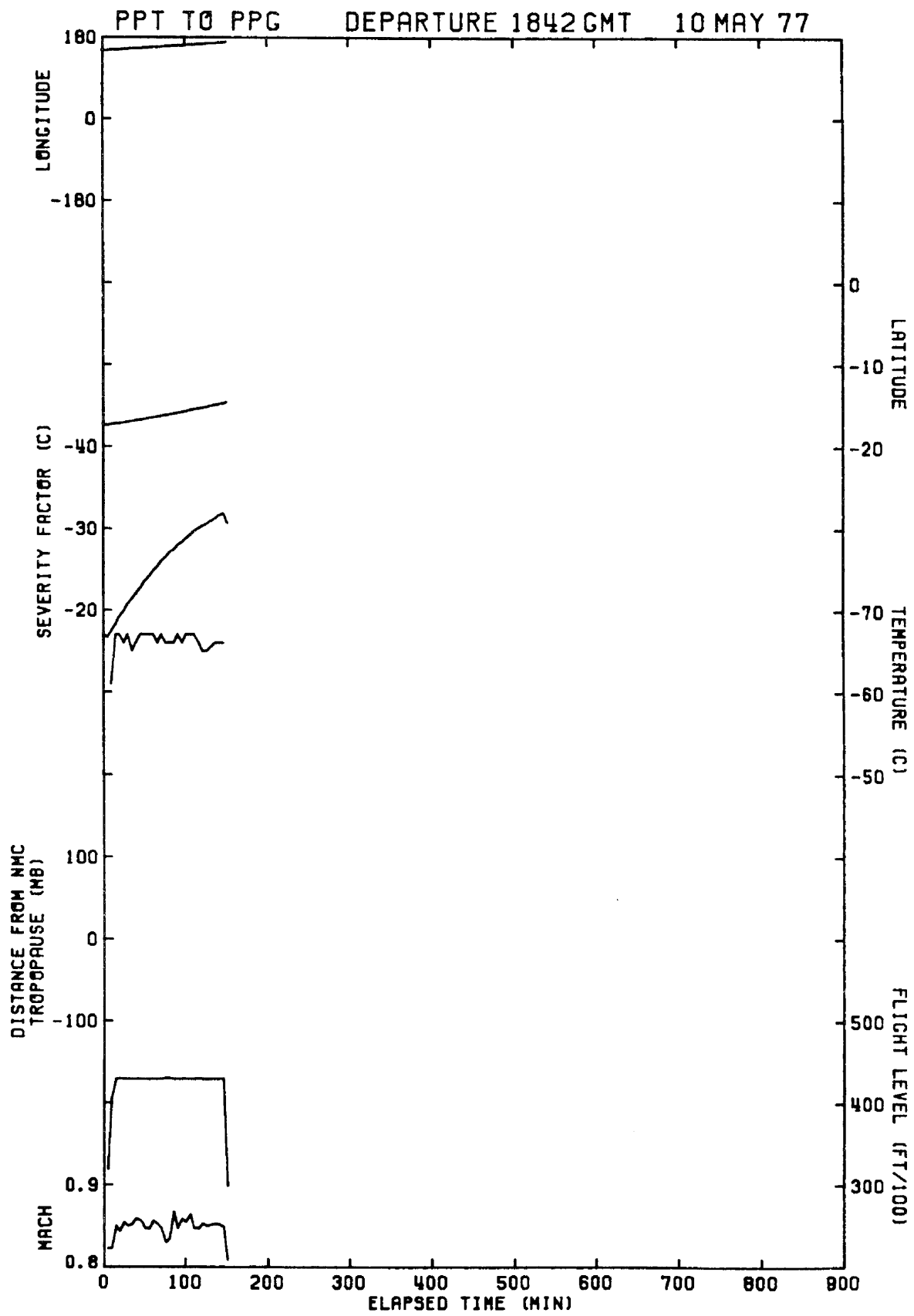


Figure 26. Flight history for flight rank 24.

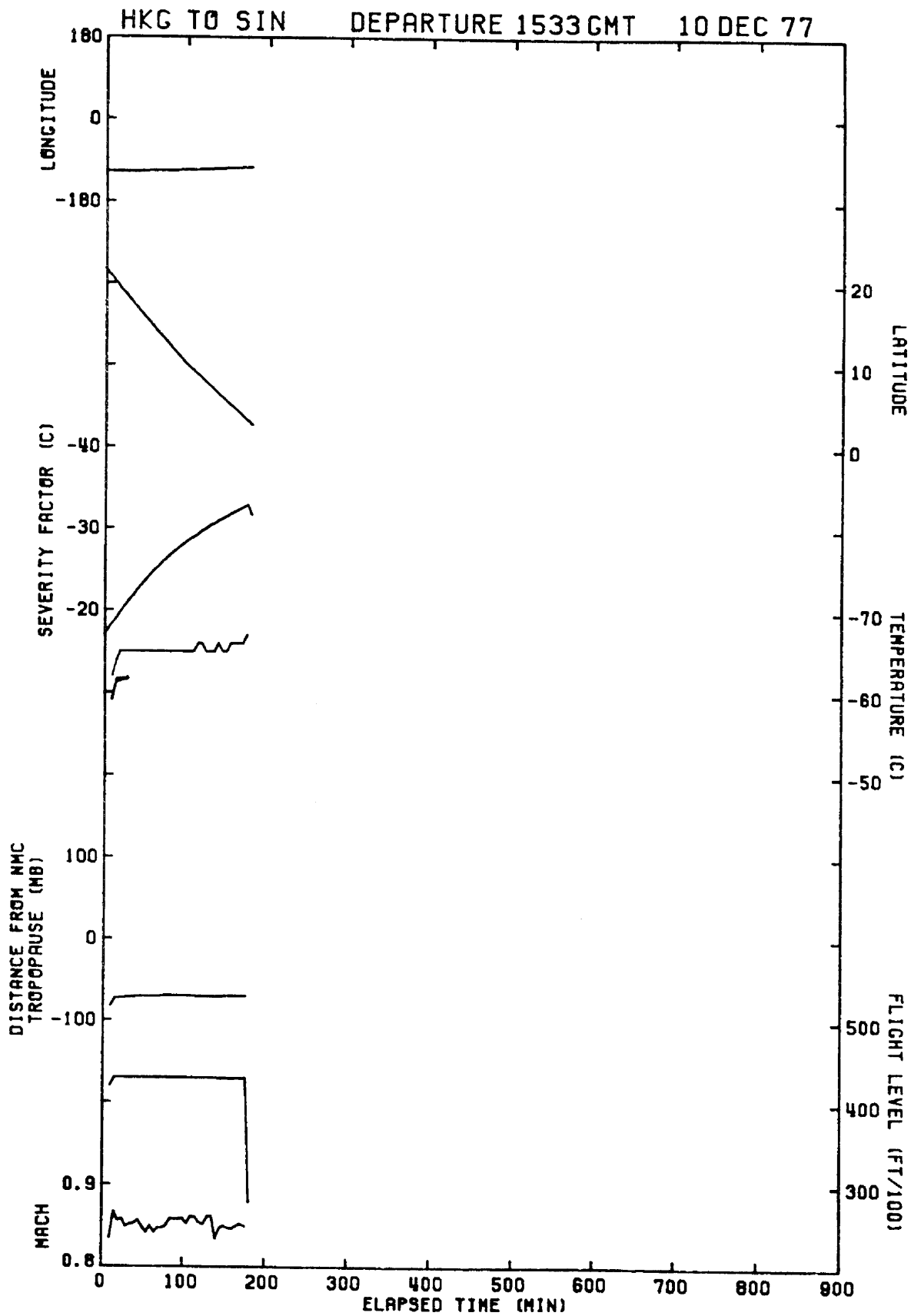


Figure 27. Flight history for flight rank 25.

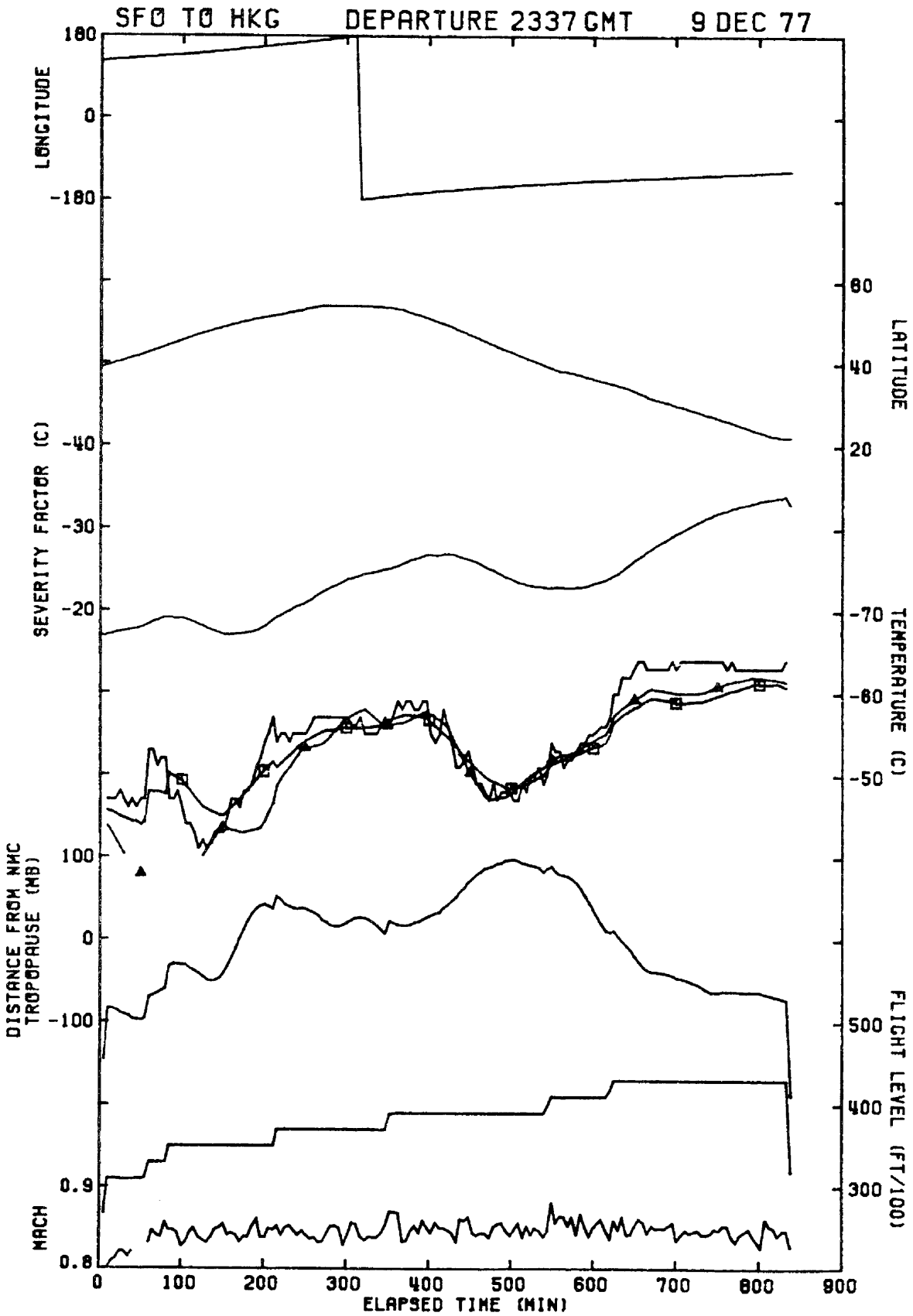


Figure 28. Flight history for flight rank 26.

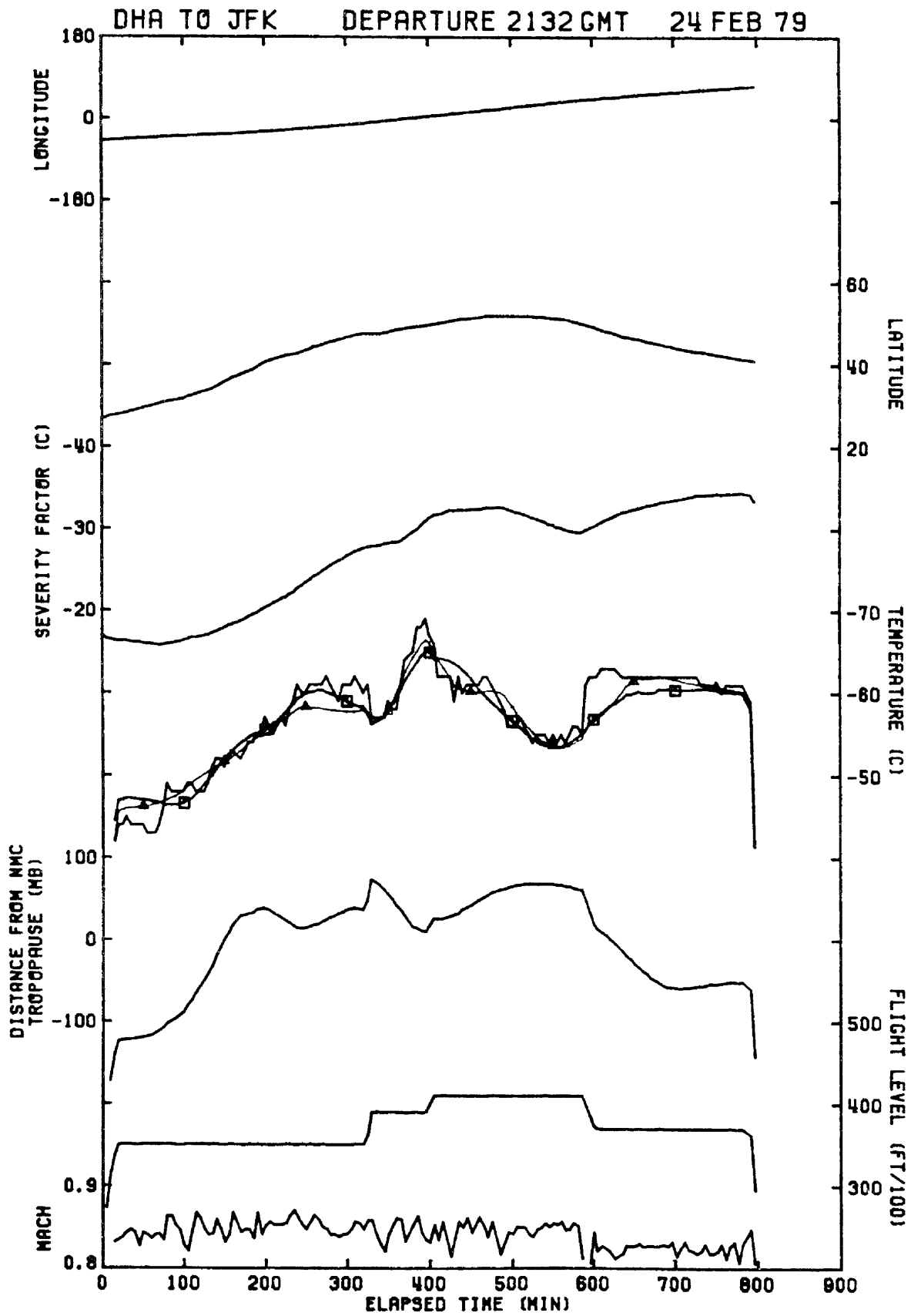


Figure 29. Flight history for flight rank 27.

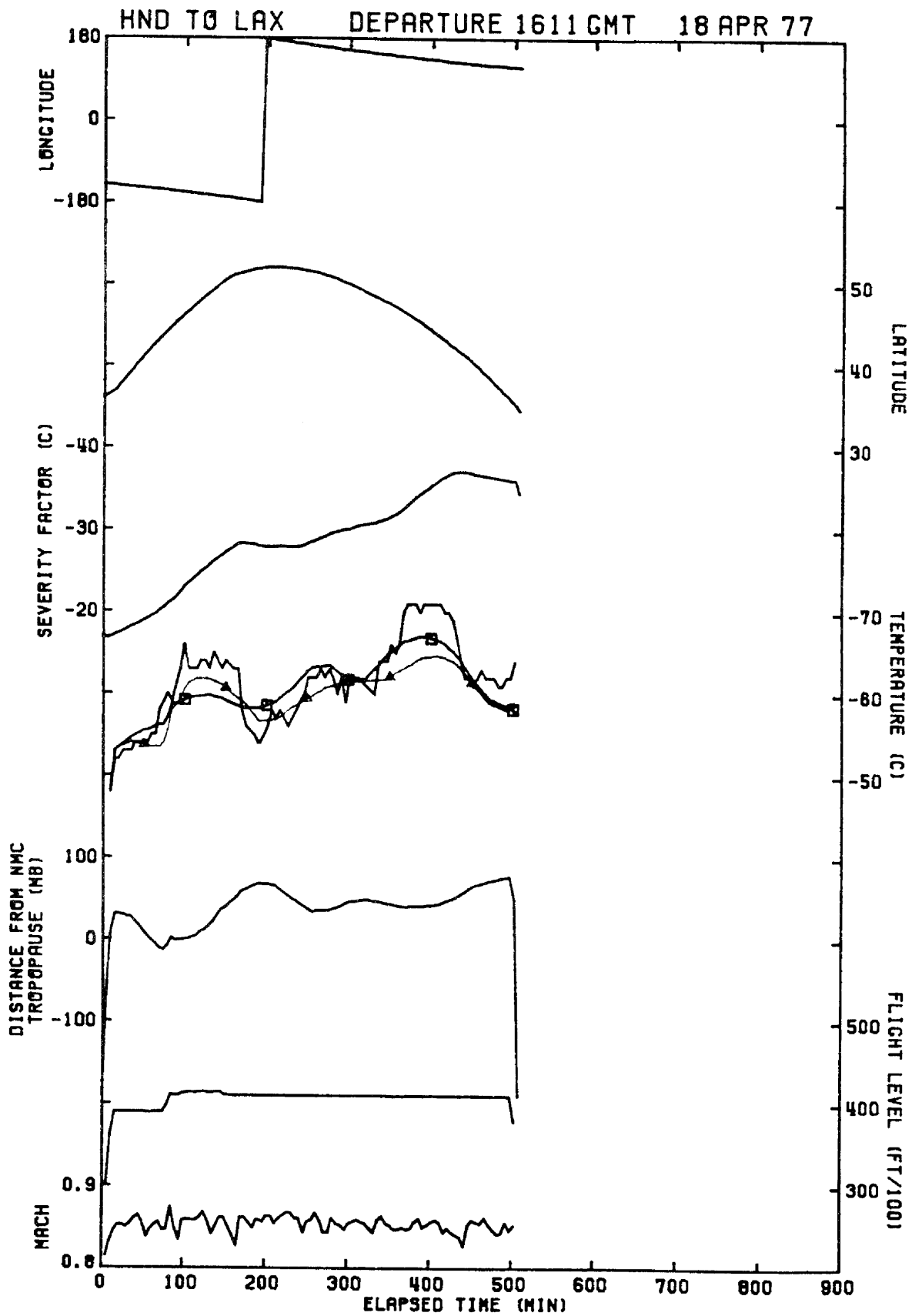


Figure 30. Flight history for flight rank 28.

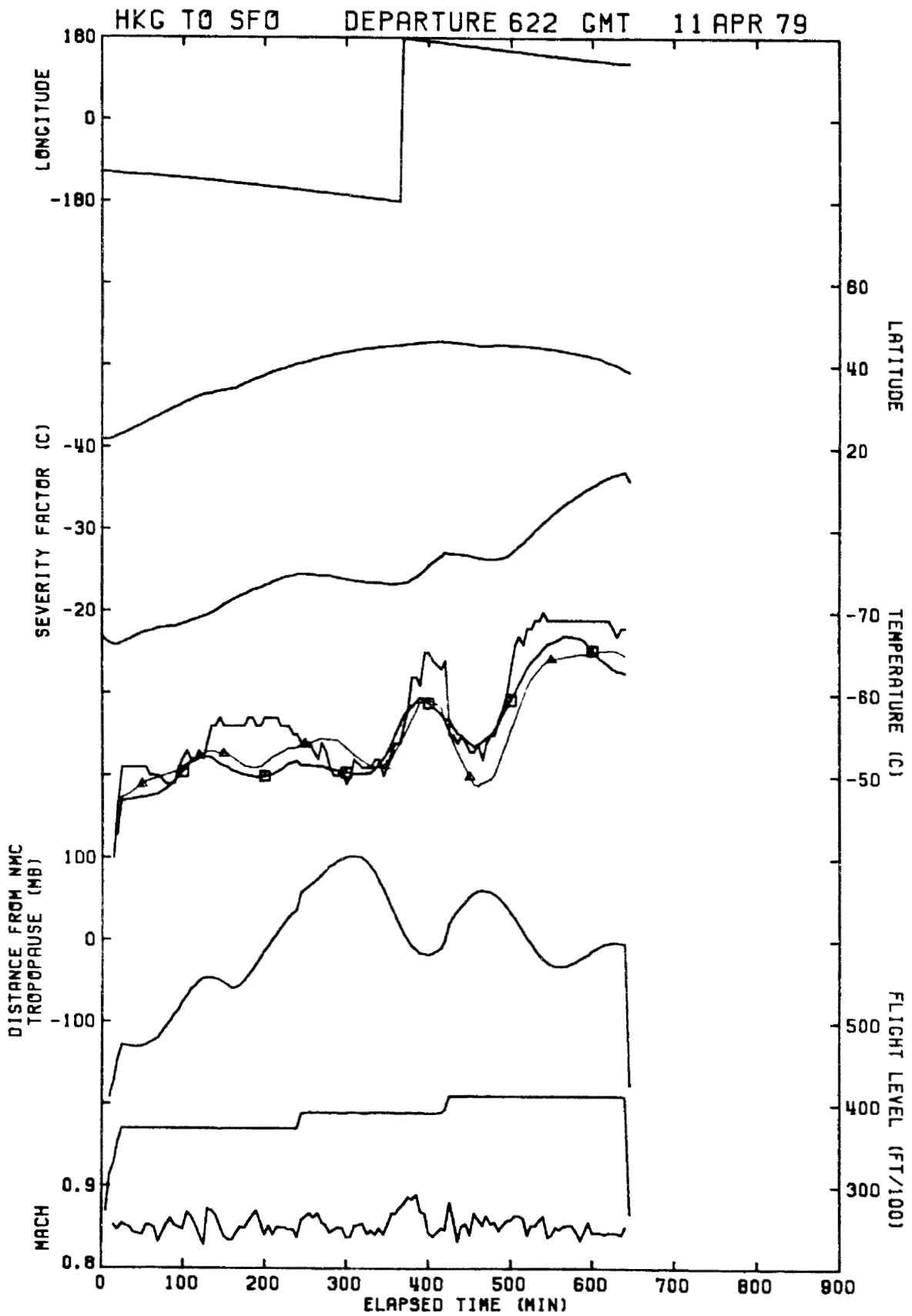


Figure 31. Flight history for flight rank 29.

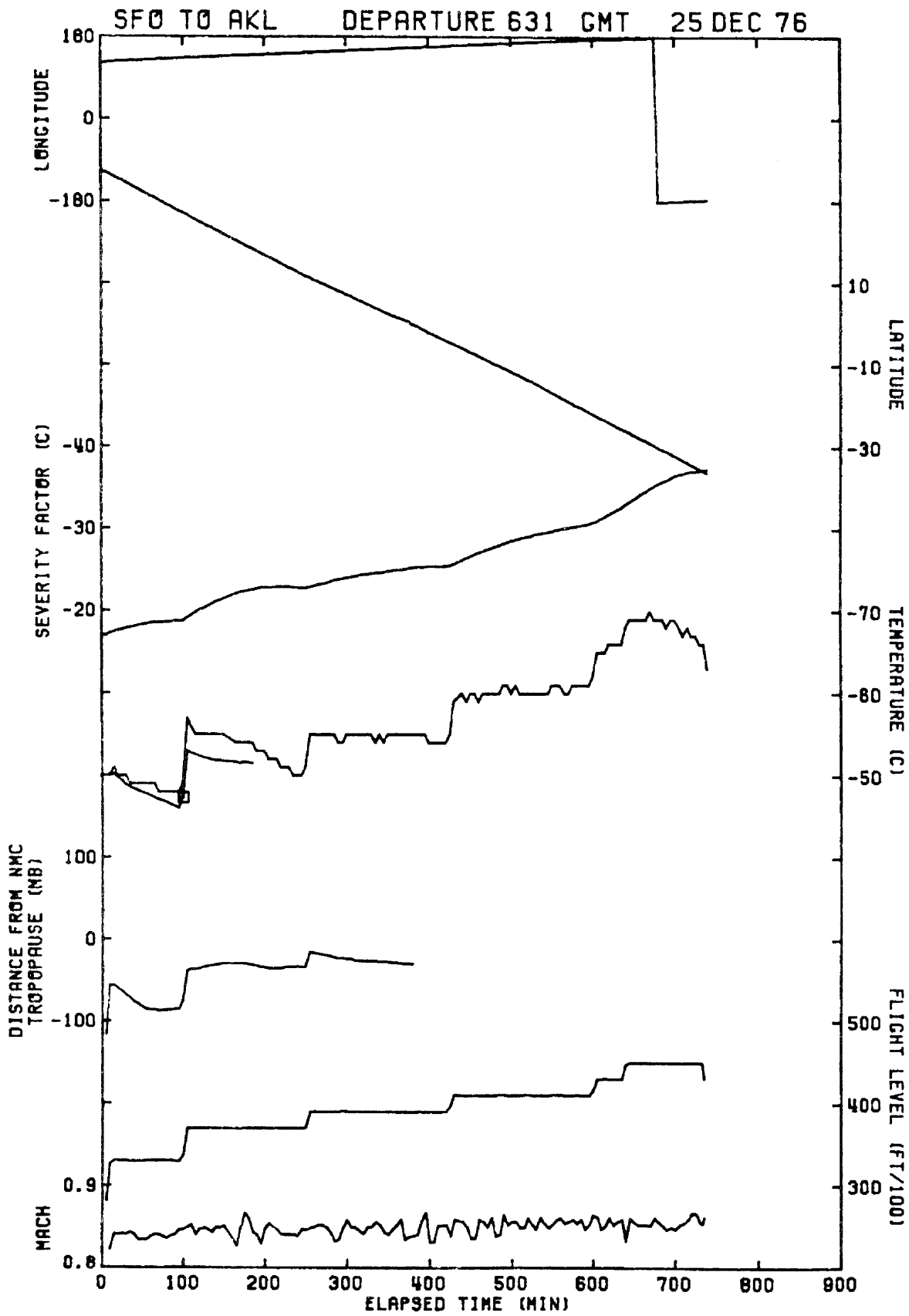


Figure 32. Flight history for flight rank 30.

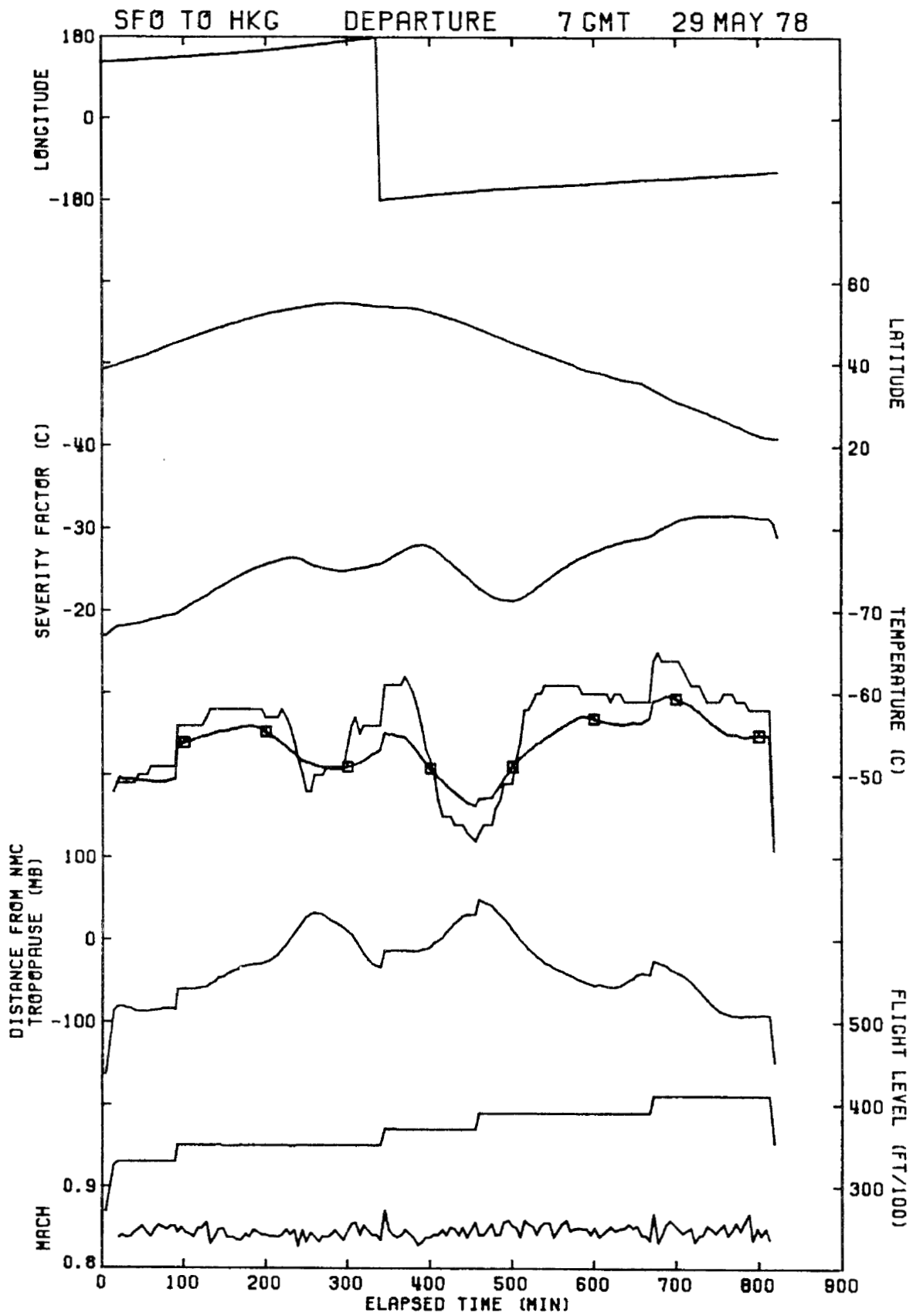


Figure 33. Flight history for flight rank 31.

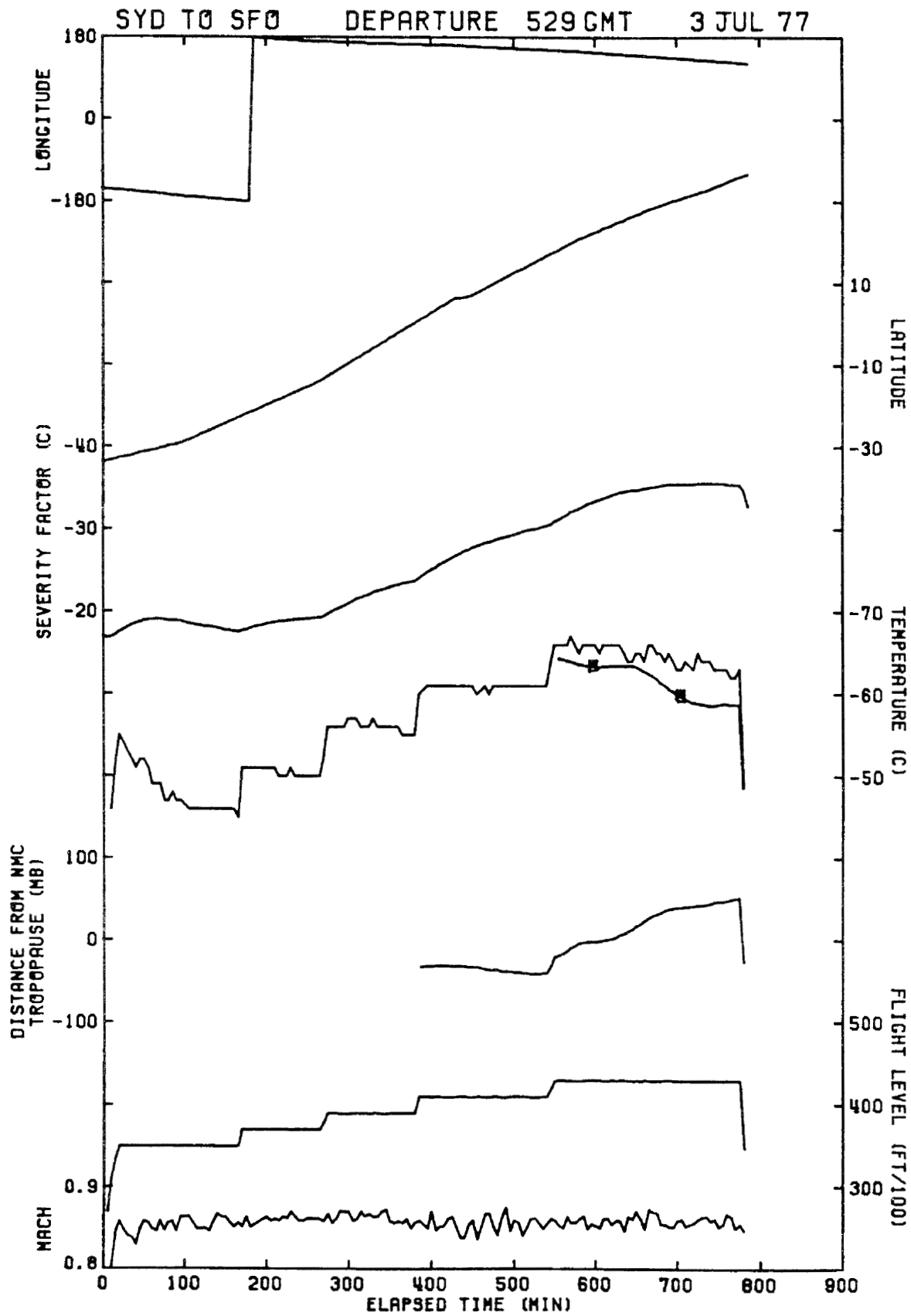


Figure 34. Flight history for flight rank 32.

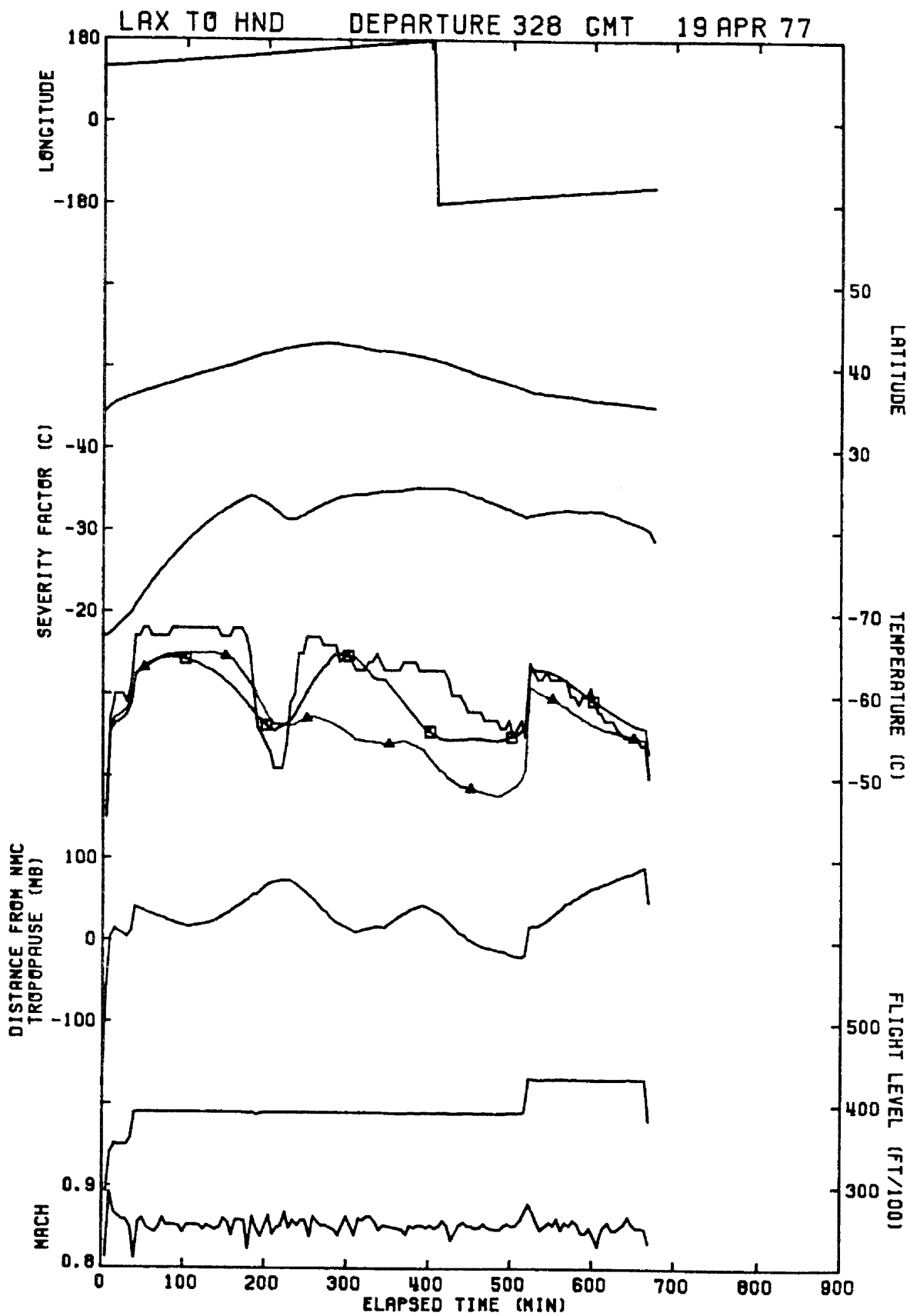


Figure 35. Flight history for flight rank 33.

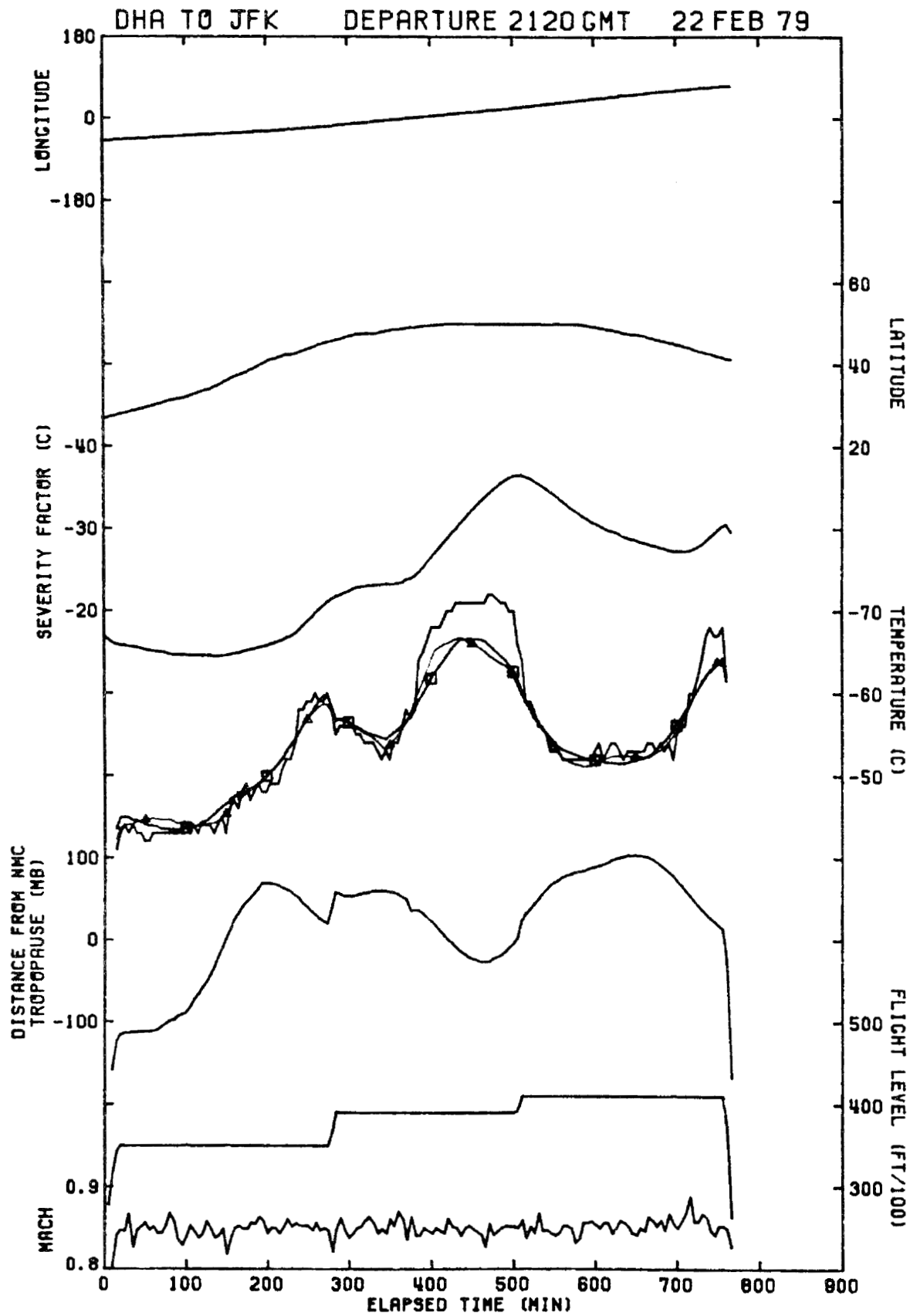


Figure 36. Flight history for flight rank 34.

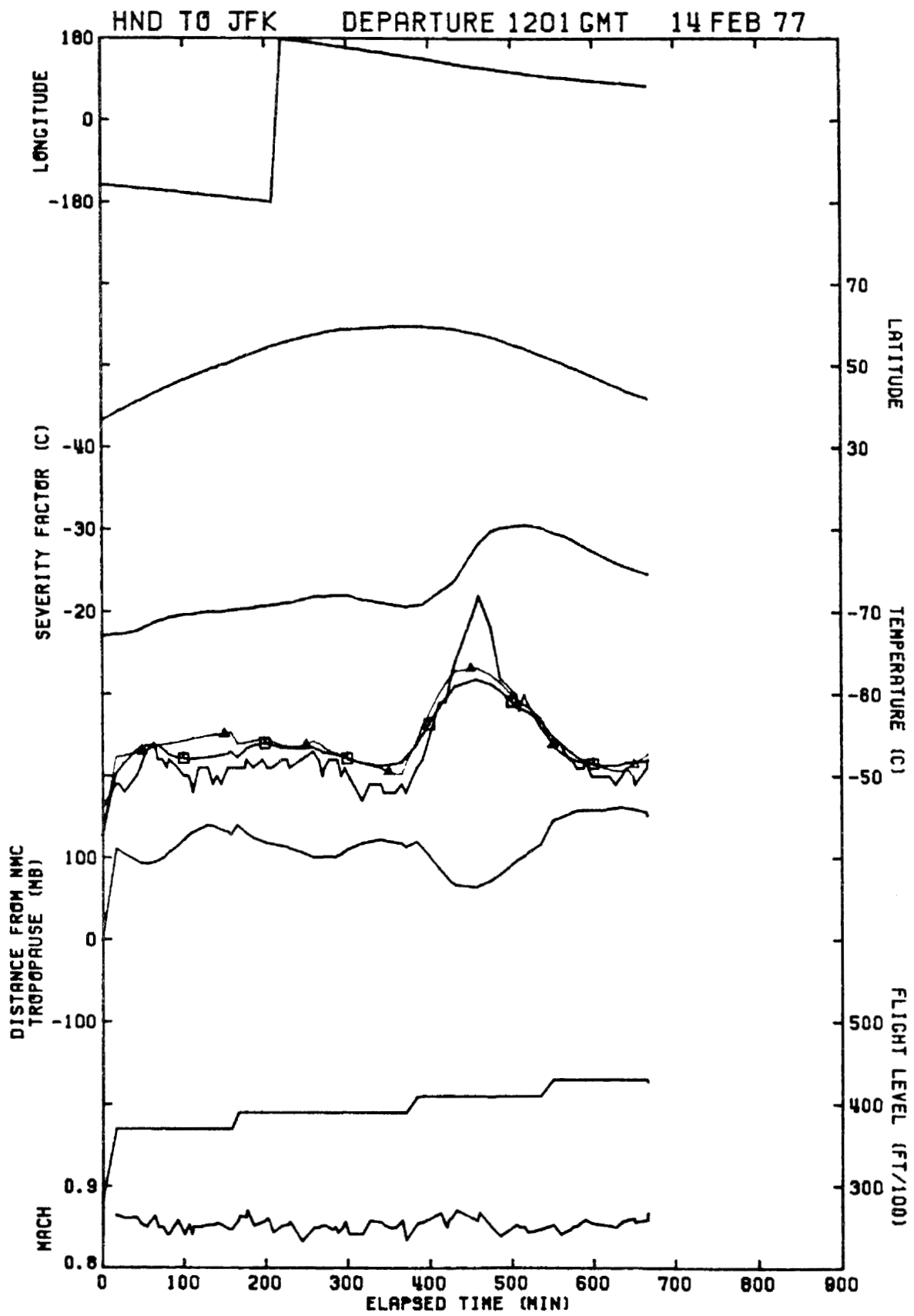


Figure 37. Flight history for flight rank 35.

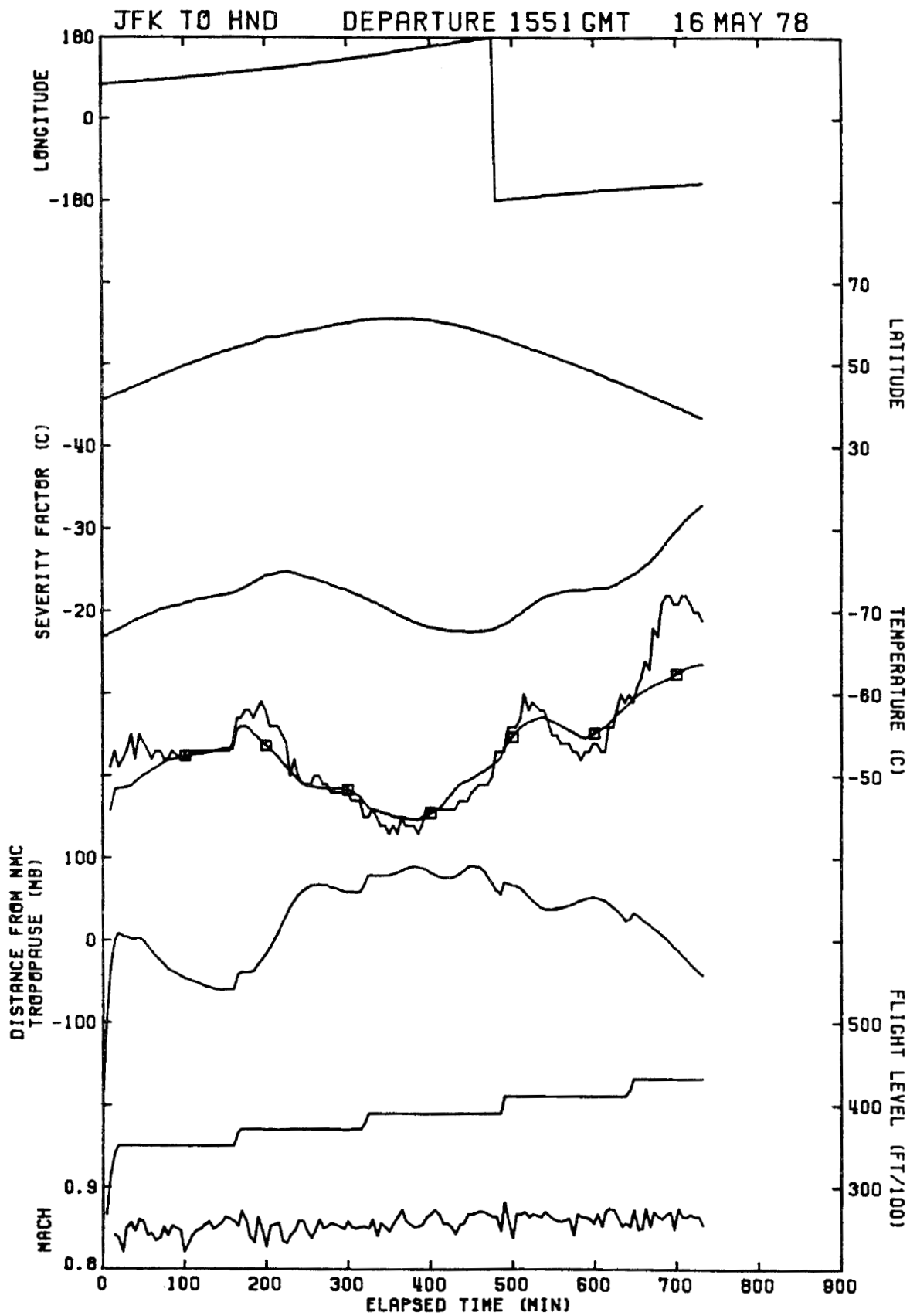


Figure 38. Flight history for flight rank 36.

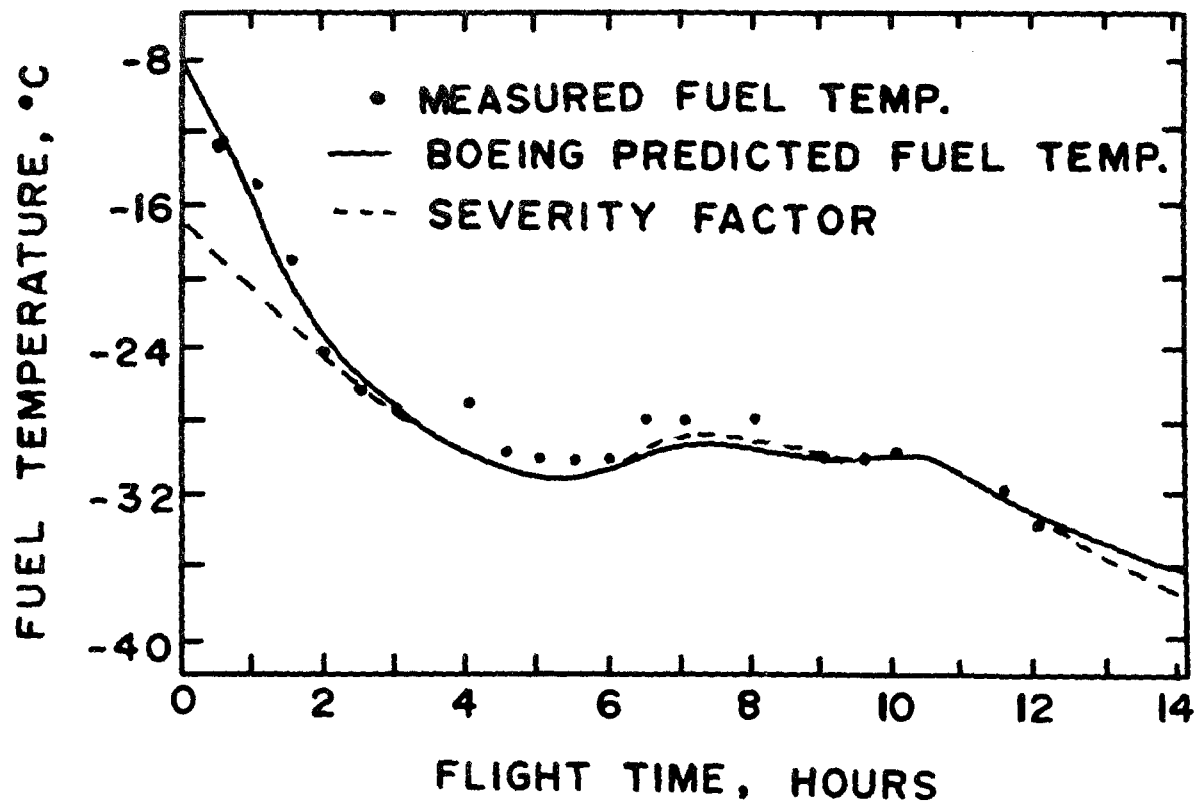


Figure 39. Comparison of calculated severity factor and Boeing-model predicted fuel temperature with measured fuel temperature on a flight from Seattle to Johannesburg.

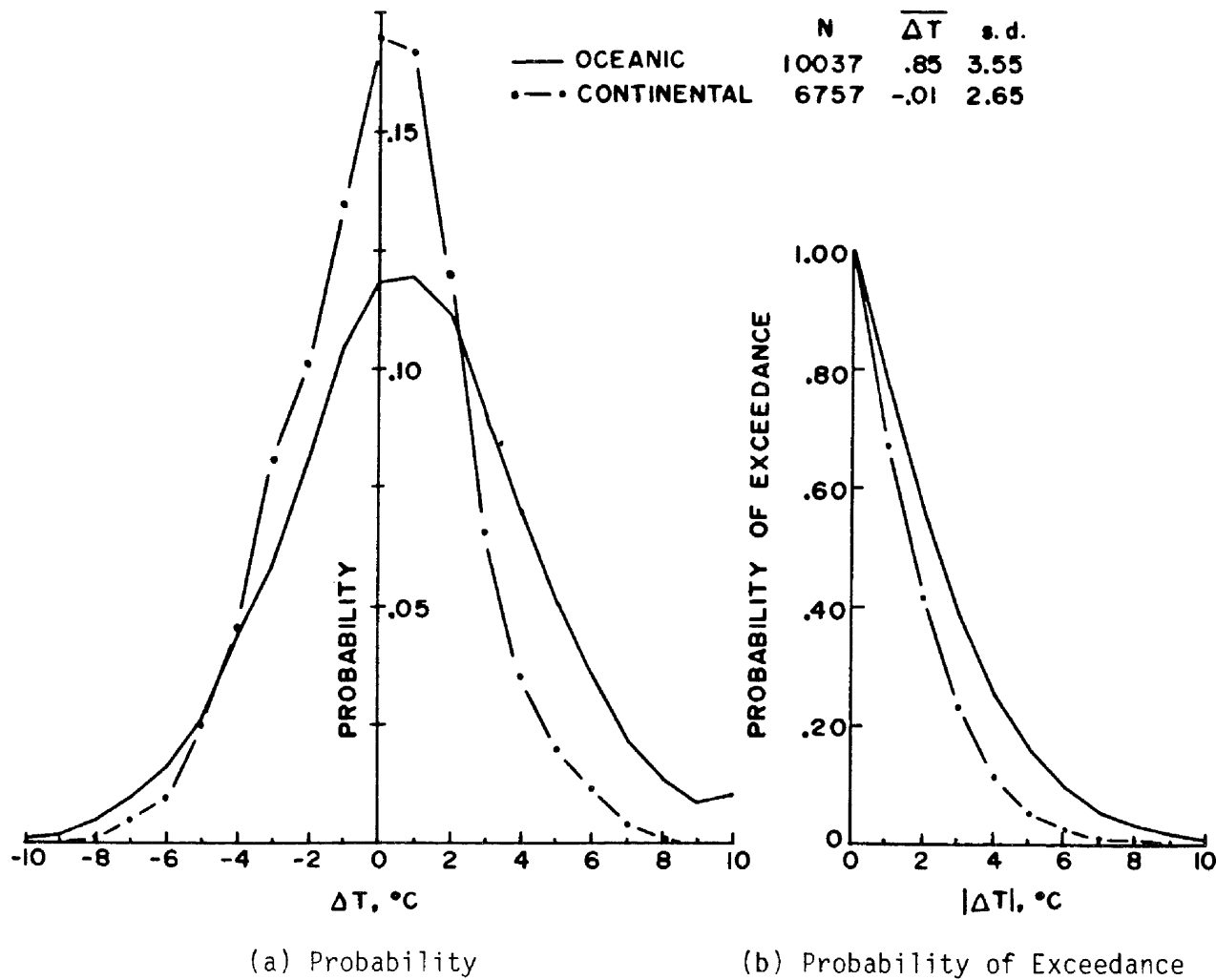


Figure 40. Distribution of differences between the GASP and NMC analysis field temperatures ($\Delta T = T_{\text{analysis field}} - T_{\text{GASP}}$) for an oceanic and a continental route. The number of observations (N), the average temperature difference ($\overline{\Delta T}$), and the standard deviation (s.d.) for each route are given in the figure.

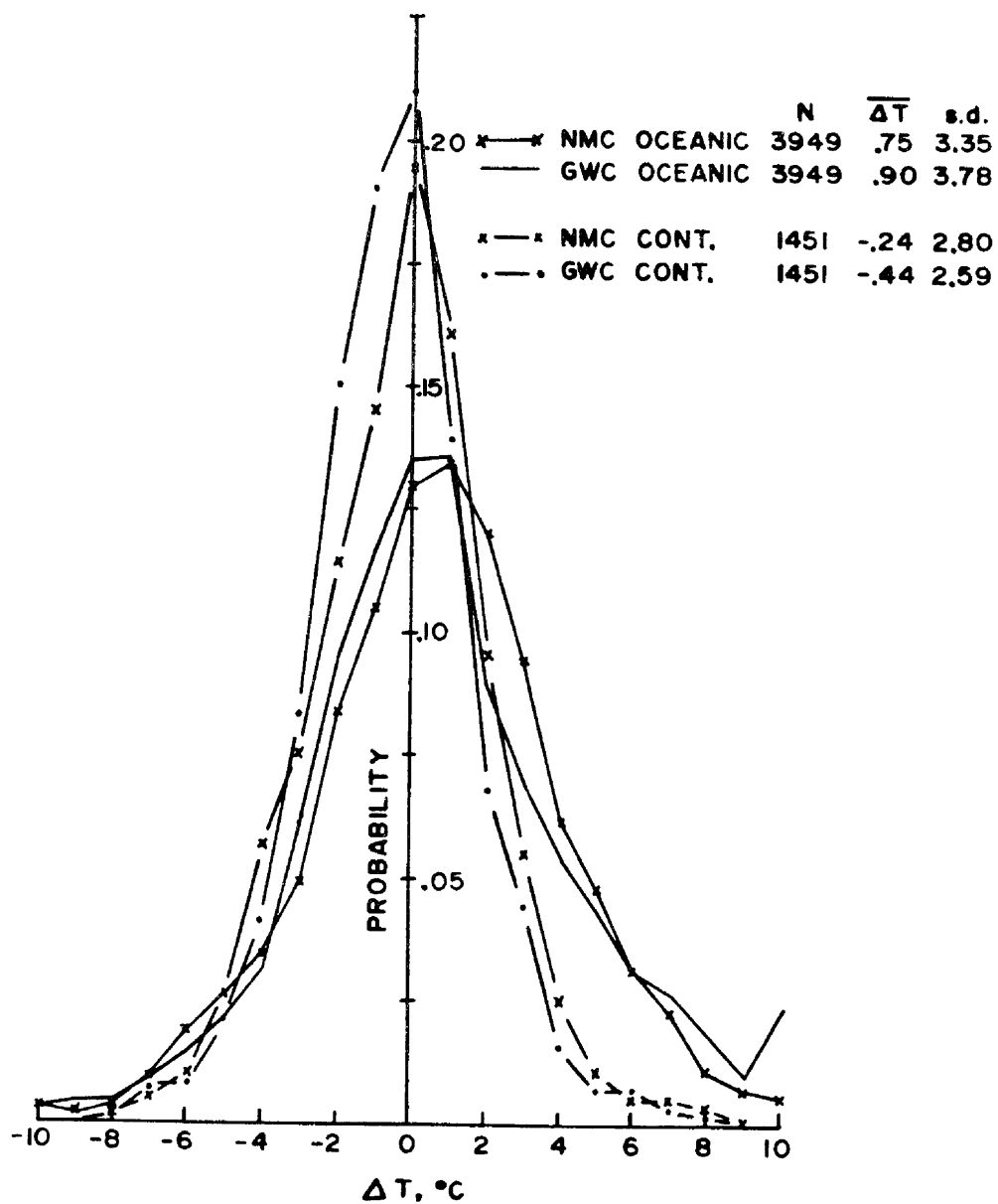


Figure 41. Distribution of differences between the GASP and the NMC and GWC analysis field temperatures ($\Delta T = T_{\text{analysis field}} - T_{\text{GASP}}$) for an oceanic and a continental route. Only observations which are common to all three data sets are included, and the number of observations (N), the average temperature difference ($\overline{\Delta T}$), and the standard deviation (s.d.) for each curve are given in the figure.

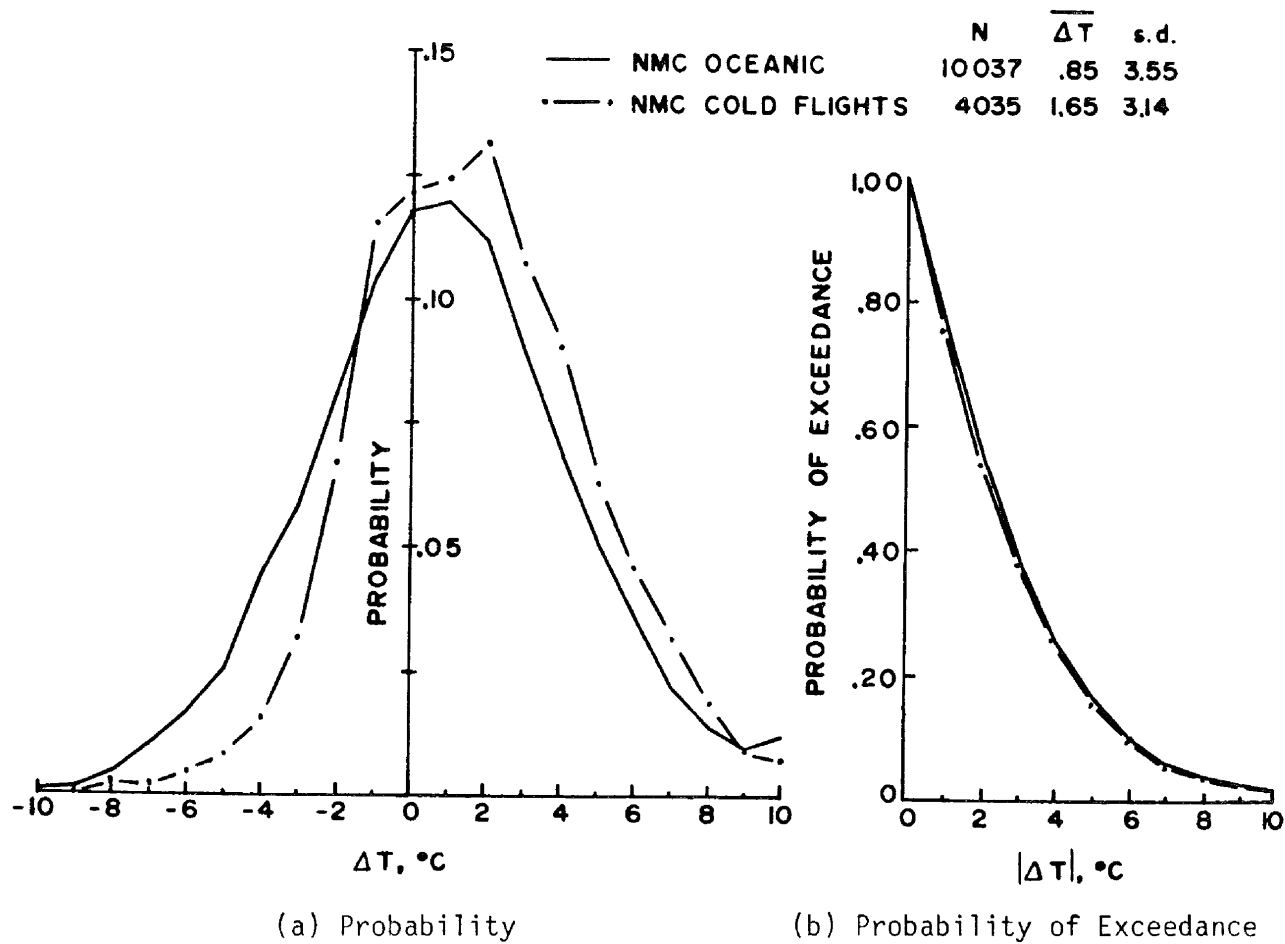


Figure 42. Distribution of differences between the GASP and NMC analysis field temperatures ($\Delta T = T_{\text{analysis field}} - T_{\text{GASP}}$) for an oceanic route and for selected extreme flights. The number of observations (N), the average temperature difference ($\overline{\Delta T}$), and the standard deviation (s.d.) are given in the figure.

1. Report No. NASA CR-168247		2. Government Accession No.		3. Recipient's Catalog No.	
4. Title and Subtitle Temperature Histories of Commercial Flights at Severe Conditions from GASP Data				5. Report Date October 1983	
				6. Performing Organization Code	
7. Author(s) W. H. Jaspersen and G. D. Nastrom				8. Performing Organization Report No. None	
				10. Work Unit No.	
9. Performing Organization Name and Address Control Data Corporation Box 1249 Minneapolis, Minnesota 55440				11. Contract or Grant No. NAS3-21249	
				13. Type of Report and Period Covered Contractor Report	
12. Sponsoring Agency Name and Address National Aeronautics and Space Administration Washington, D.C. 20546				14. Sponsoring Agency Code 535-06-12	
15. Supplementary Notes Final report. Project Manager, Robert Friedman, Aerothermodynamics and Fuels Division, NASA Lewis Research Center, Cleveland, Ohio 44135.					
16. Abstract <p>This report is a study of the thermal environment of commercial aircraft from a data set gathered during the Global Atmospheric Sampling Program (GASP). The data set covers a four-year period of measurements. The report presents plots of airplane location and speed and atmospheric temperature as functions of elapsed time for 36 extreme-condition flights, selected by minimum values of several temperature parameters. One of these parameters, the severity factor, is an approximation of the in-flight wing-tank temperature. Representative low-severity-factor flight histories may be useful for actual temperature-profile inputs to design and research studies. Comparison of the GASP atmospheric temperatures to interpolated temperatures from National Meteorological Center and Global Weather Central analysis fields shows that the analysis temperatures are slightly biased toward warmer than actual temperatures, particularly over oceans and at extreme conditions.</p>					
17. Key Words (Suggested by Author(s)) Atmospheric temperature; Aircraft fuels; Aircraft measurements; Fuel temperature; Temperature climatology			18. Distribution Statement Unclassified - unlimited STAR Category 03		
19. Security Classif. (of this report) Unclassified		20. Security Classif. (of this page) Unclassified		21. No. of Pages 63	22. Price* A04

* For sale by the National Technical Information Service, Springfield, Virginia 22161